

1 **Prolonged landscape stability sustained the continuous development**
2 **of ancient civilizations in the Shuangji River valley of China's Central**
3 **Plains**

4 Peng Lu^{a,b,*}, Junjie Xu^{c,l}, Yijie Zhuang^{d,**}, Panpan Chen^{a,b}, Hui Wang^{e,**}, Yan Tian^{a,b}, Duowen
5 Mo^{a,f}, Wanfa Gu^g, Ruixia Yang^b, Xia Wang^{a,b}, Liang Zhou^h, Yongqiang Li^e, Xiaohu Zhangⁱ, Ye Li^{a,b}

6

7

8 ^a Institute of Geography, Henan Academy of Sciences, Zhengzhou, 450052, China

9 ^b Zhengzhou Base, International Center on Space Technologies for Natural and Cultural Heritage
10 under the Auspices of UNESCO, Zhengzhou, 450052, China

11 ^c College of History, Zhengzhou University, Zhengzhou, 450000, China

12 ^d Institute of Archaeology, University College London, London, WC1H 0PY, UK

13 ^e The Institute of Archaeology, Chinese Academy of Social Sciences, Beijing, 100710, China

14 ^f Laboratory for Earth Surface Processes, Ministry of Education, College of Urban and
15 Environmental Sciences, Peking University, Beijing, 100871, China

16 ^g Zhengzhou Municipal Institute of Cultural Relics and Archaeology, Zhengzhou 450000, China

17 ^h School of Geography, Geomatics, and Planning, Jiangsu Normal University, Xuzhou 221116,
18 China

19 ⁱ Henan Provincial Institute of Cultural Relics and Archaeology, Zhengzhou, 450000, China

20

21

22 *Corresponding author. Institute of Geography, Henan Academy of Sciences, Zhengzhou, 450052,

23 China

24 **Corresponding authors.

25 E-mail: bulate_0@163.com (P. Lu), y.zhuang@ucl.ac.uk (Y. Zhuang), wh@cass.org.cn (H. Wang).

26 ¹ P.L. and J.X. contributed equally to this study.

27

28 **Abstract:** The continuous development of the Neolithic to Bronze-Age cultures on China's Central
29 Plains is well contested by archaeological and historical research. Environmental factors that
30 sustained such an exceptionally long cultural continuity are, however, poorly understood. The
31 evolution of fluvial landscapes and its relationship with cultural developments are key to disentangle
32 the close interaction between the environment and civilizational discourse on the Central Plains.
33 Here, we present OSL and AMS 14C ages and other environmental data collected from a range of
34 typical geomorphological locations in the Shuangji River valley, which is situated at the heartland
35 of the Central Plains and long considered to be one of the most important regions for the rise of the
36 Chinese civilization. Combining the OSL and 14C dates, results of particle size and soil/sediment
37 micromorphological analyses, and geoarchaeological field observations, we reconstructed the
38 evolution of Holocene geomorphological landscape in the Shuangji River valley. The results show
39 that the Neogene alluvial fan was incised into a wide valley during the early Pleistocene. Subsequent
40 alluvial processes were constrained within this general framework of regional landform. The period
41 of 20 ka BP and 10-8 ka BP saw two episodes of basin-scale alluvial incision, which created two
42 alluvial terraces (i.e., T4 and T3), respectively. Despite the occurrence of episodic floods and some
43 large-scale alluvial siltation during 8-3 ka BP, the alluvial surfaces remained stable for a prolonged

44 period of time and thus provided optimal living conditions for prehistoric inhabitation. We argue
45 that the geomorphological foundation and prolonged landscape stability were instrumental to the
46 continuous cultural developments on the Central Plains as seen in the Shuangji River valley as a
47 representative of such long-term human-environment interactions. Our geoarchaeological survey
48 for the first time reveals basin-scale evidence on the mechanism responsible for this distinctive
49 relationship between alluvial landscape and cultural development, in which the terrace-surface
50 stability, alongside many other cultural factors, profoundly shaped the celebrated cultural continuity
51 on prehistoric Central Plains.

52

53 **Keywords:** Shuangji River, geomorphology, landscape, Central Plains, cultural continuity

54

55

56

57

58

59

60

61

62

63

64

65

66 **1. Introduction**

67 In alluvial geoarchaeology, basin-scale reconstruction of palaeo-environment and landscape
68 evolution is vital to our understanding of long-term and multi-scalar interactions between cultural
69 successions and environmental fluctuations (Kidder et al, 2008, 2012, 2015; Zhuang and Kidder ,
70 2014). Alluvial basins provide essential natural resources for cultural developments. The ways how
71 humans organize their settlements, produce food, and interact with one another are therefore
72 inherently influenced by the altitude, landform, climate, and many other physical properties of
73 alluvial basins (Brown, 1997). Because of this, basin-scale human-environmental dynamics
74 contribute significantly to the shaping of civilizational discourses under different alluvial settings.
75 For instance, Kidder et al. (2008) found that the Upper Tensas Basin of the Lower Mississippi River
76 which is characterized by a prolonged stability of alluvial landscapes but with several episodes of
77 significant river readjustments, as revealed by recent geoarchaeological surveys, is closely
78 associated with prehistoric and historical cultural developments in the basin for the past 10,000
79 years. Similarly, the recent systematic basin-wide survey and reconstruction of the Holocene alluvial
80 landscape of the Upper Nile have shed fresh insights into the responses of Holocene fluvial
81 environments to climate change and how they affected human adaptations (Macklin et al, 2013,
82 2015). The importance of demonstrating the long-term development of fluvial landscapes to a more
83 rigorous evaluation of prehistoric cultural adaptations can be also seen in Giosan and colleagues’
84 recent study (2012) which reconsiders the classical issue of the collapse of the Harappan civilization
85 through their robust reconstruction of the late-Holocene fluvial landscape in the region. Some of the
86 findings allowed by these geoarchaeological surveys are significantly different from previous
87 suggestions on societal responses (e.g., succession of the Kerma Kingdom) to climate change, which

88 tend to hold a simplistic, one-sided perspective. Instead, these new studies promote a holistic
89 understanding of the importance of geomorphological condition (e.g., stabile alluvial landscapes) to
90 cultural succession, resilience and adaptation.

91 Large river basins across China, including notably the different catchments of the Yellow River,
92 Yangtze River, and the Western Liao River, sustained the prosperity of multiple prehistoric cultures
93 and civilizations (Yan, 1987; Su, 2009; Liu and Chen, 2017). Compared to other civilizational
94 regions such as the Lower Yangtze River which experienced dramatic rise and fall of early
95 civilizations (Yu et al, 2000; Zheng et al, 2021; He et al, 2021), the Central Plains region in the
96 Middle and Lower Yellow River valleys was one of the few regions where prehistoric cultures
97 developed continuously without an obvious hiatus (Liu and Han, 2016). Such a cultural continuity
98 eventually fostered the emergence of early cities and state-level polities on the Central Plains which
99 is widely considered one of the most important regions for the origin of the Chinese Civilization.
100 Amongst the factors that sustained this unique civilizational discourse on the Central Plains, the
101 physical environment and its characteristics played an instrumental role (Zhou et al, 2005). While
102 long-term climate change has a profound impact on the overall patterns and characteristics of
103 cultural developments (Yu et al, 2020), it is the specific geomorphological conditions that define
104 how humans adapt to different environmental settings and climate regimes (Macklin et al, 2015).
105 Specifically, settlement patterns and subsistence strategies of prehistoric cultures in the region are
106 intrinsically constrained by altitude, topographic undulation, and hydrology of the alluvial
107 environments (Lu et al, 2013a, 2017).

108 The vast Central Plains region in fact includes a diverse range of landscapes and environments.
109 As one of the regions that has received most intensive archaeological quest for the origin of Chinese

110 civilization, the Shuangji River valley of the Central Plains provides an ideal case to investigate how
111 the growth and flourishing of prehistoric settlements were intricately related to the evolution of
112 Holocene geomorphological landscapes of the river basin (Zhang ZY, 2007). Recently, several
113 studies have investigated the relationship between the Holocene environment and cultural
114 development in the Shuangji River. Zhang ZY et al. (2007) proposed that, confined by the narrow
115 river valleys on shallow geological outcrops, most Yangshao culture and later Neolithic sites were
116 situated on the alluvial terraces (T2) or further high up on the loess tablelands in the region. Whilst
117 one might assume that, according to Zhang ZY et al.'s suggestion, these Neolithic sites might be
118 free from the impact of floods, Xia et al. (2003) found flood deposits embedded on the oldest and
119 highest-elevation alluvial terraces (T4) and thus suggested that the flood occurred during the 3550-
120 3400 BP. If this was indeed the case, it would mean that these places were once inundated in flood
121 water. According to Wang H (2007, 2019), an event of alluvial aggradation occurred between 5000-
122 2500 BP in Shuangji River. Based on these studies, Lu (2017, 2019b) and colleagues further
123 proposed three episodes of alluvial accretion and incision that took place between 10000-9000 BP,
124 9000-4000 BP, and 4000-historical times, respectively in the Shuangji River region. More
125 chronological data and a more accurate chronological framework are required to refine these
126 reconstructions on the evolution of the Holocene geomorphological landscape in the Shuangji River
127 valley, especially the duration and mechanism of its prolonged stability. More importantly, synthetic
128 studies are needed to further understand why prehistoric settlements were concentrated on the loess
129 tablelands and alluvial terraces, how such a prolonged landscape stability supported continuous
130 cultural developments in the Shuangji River valley of the Central Plains, and if such human-alluvial
131 landscape dynamics represented a distinctive model of prehistoric cultural adaptation in China.

132 We present results from our geomorphological and geoaerchaeological surveys in the Shuangji
133 River valley and reconstruct evolution of Holocene geomorphological environments using high-
134 resolution chronological and environmental data. Our results highlight the close relationship
135 between the cultural continuity and landscape stability in the basin and shed new lights to understand
136 how long-term geomorphological evolution facilitated the unparalleled cultural continuity on
137 prehistoric Central Plains and evaluate the environmental foundation to this unique discourse to the
138 rise of early civilizations in China.

139 **2. Geographical setting and archaeological backgrounds**

140 The Shuangji River valley is situated in the middle part of the Central Plains. The river
141 originates from the low mountainous area to the northeast of the Songshan Mountain range. It flows
142 through a diverse range of terrains from northwest to southeast, including mountains, loess
143 tablelands and alluvial plains. The entire length of the river channel is around 171km, and the whole
144 catchment covers an area of > 1800km² (Figure 1). The region belongs to the temperate continental
145 climate zone with an average annual temperature of around 15°C and an average annual precipitation
146 of around 600mm. Controlled by the Songshan Uplift, the regional topography is high on the
147 northwest and low on the southeast, with the altitude undulating between 110-180 m above sea-
148 level. The sediments in the valley mainly consist of wind-blown loess accumulated during the
149 Quaternary era. Loess deposited during the Late Pleistocene is most widespread, whilst loess of the
150 middle Pleistocene age can be also seen in some areas. Tertiary red clay is exposed on some higher-
151 altitude locations of the region. The Shuangji River channel cuts out a deep (15-30 m) and wide
152 (200 m) northwest-southeast running valley on flat loess tablelands. Similarly, some other small
153 tributaries such as the Zhenshui River and the Huangshui River also create deeply (10-20 m) incised

154 valleys on the loess landscape.

155

156

157

158

159

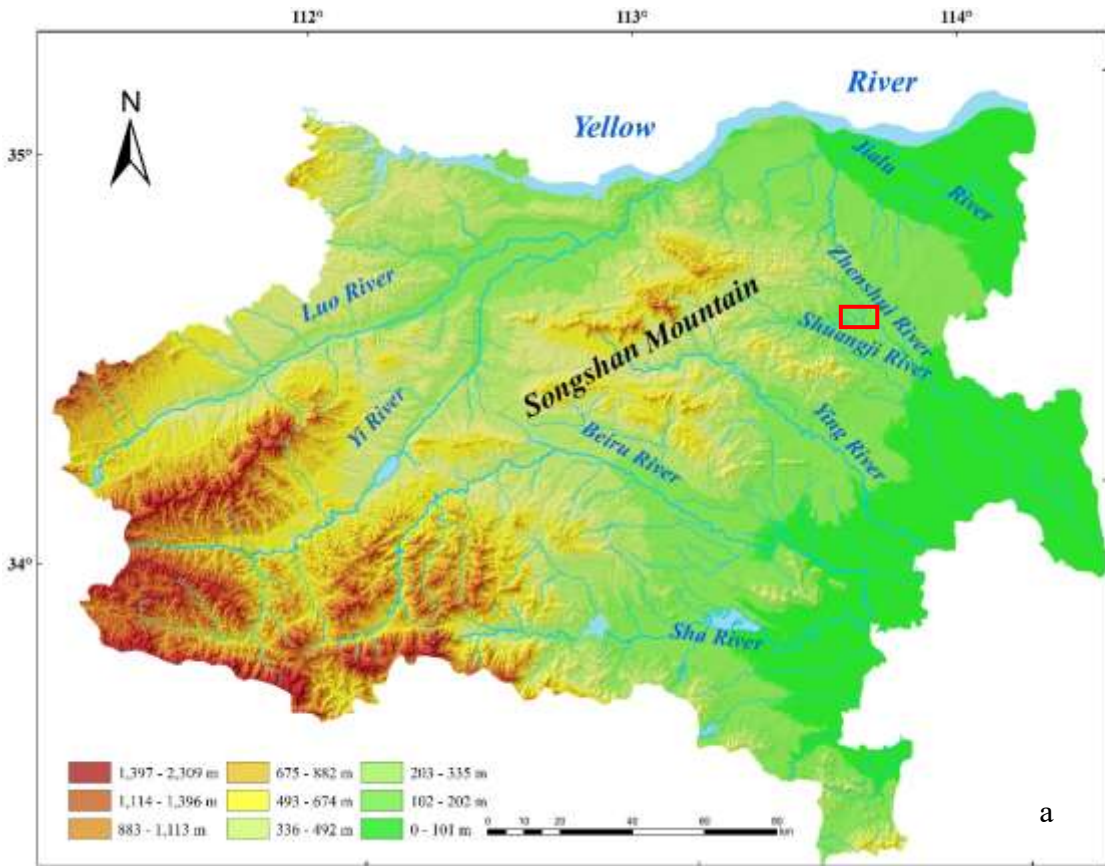
160

161

162

163

164



a

165

166

167

168

169

170

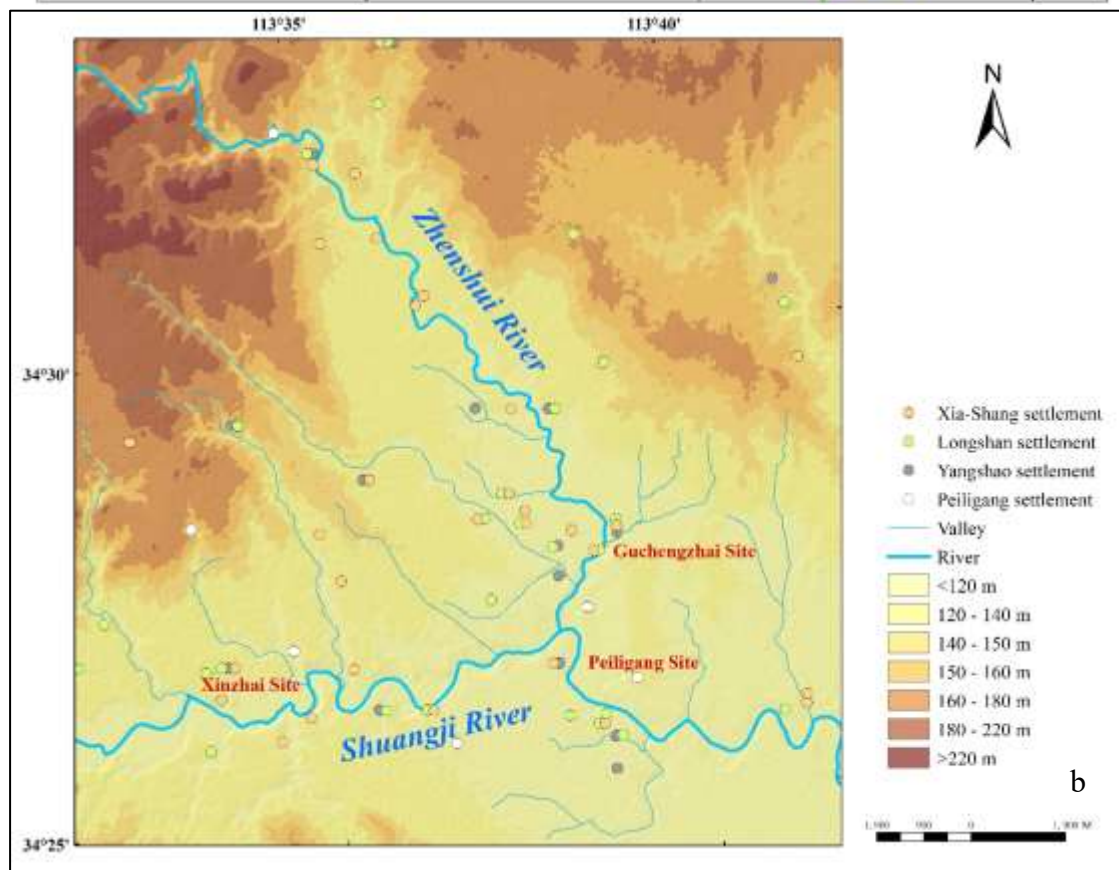
171

172

173

174

175



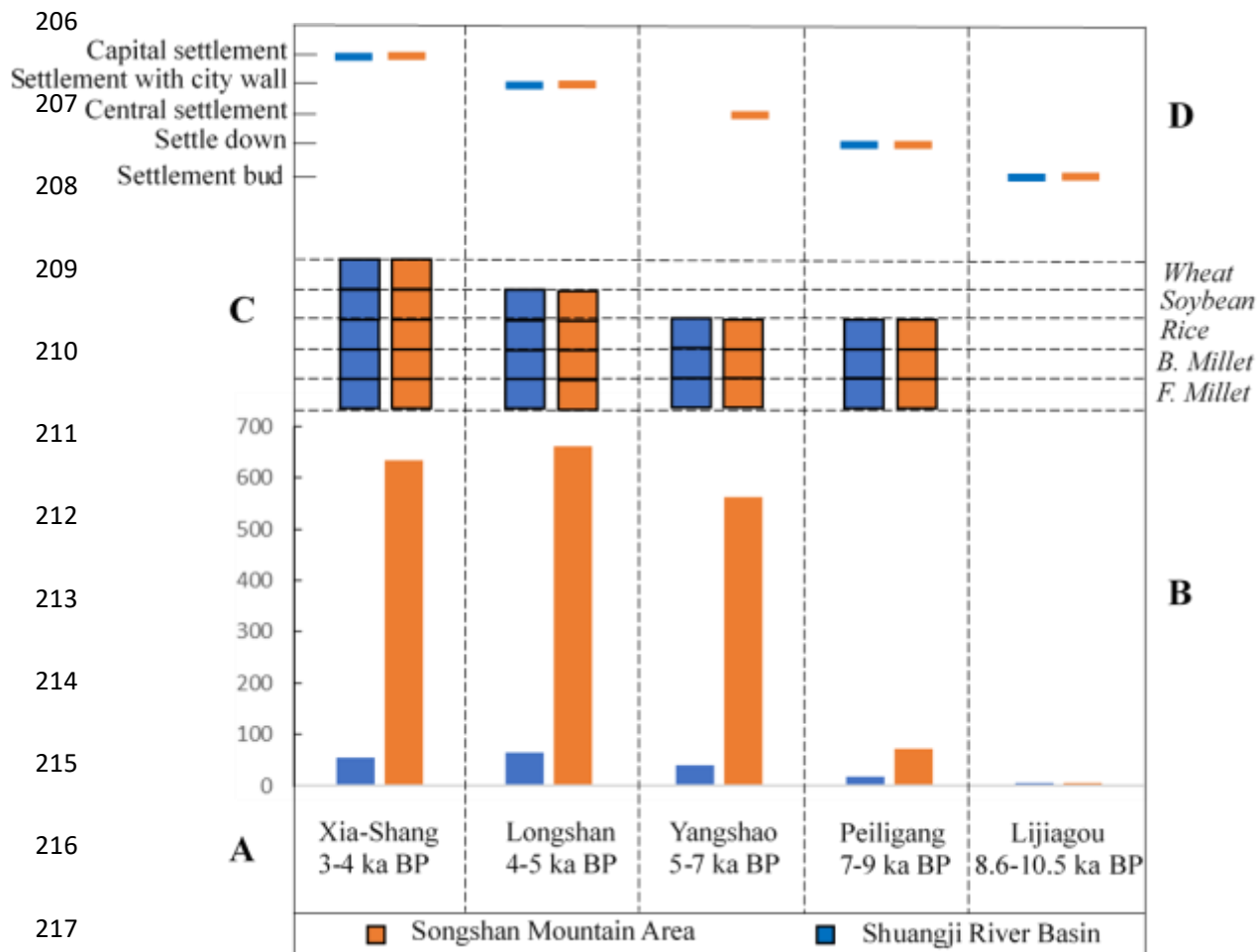
b

176 Figure 1. Geographic location of the studied region. a. Location of the Shuangji River valley (red
177 rectangular) in the Songshan Mountain Region. b. The terrain, water system and distributions of
178 prehistoric settlements of the Shuangji River valley.

179

180 Despite of a relatively small river, the Shuangji River valley has sustained continuous
181 development of prehistoric cultures. This continuity is parallel with the prosperous prehistoric
182 cultural sequence on the broad Central Plains region (Figure 2). As early as the Palaeolithic period,
183 human activities were already active in the region and from the early Neolithic period, sedentary
184 settlements began to emerge (Wang YP, 2013). The earliest Neolithic culture on the Central Plains,
185 the Lijiagou site (ca.10500-8600 BP), was located in the Shuangji River valley (Wang YP et al,
186 2011). Since the Peiligang culture period (ca. 9000-7000 BP), settlements began to mushroom
187 across the region, making it a region with the highest population density in the contemporary Central
188 Plains. The settlements were, however, of small scale and there was no clear hierarchical difference
189 between them (Lu et al, 2013b, 2019a; Li YQ et al, 2020). The settlement growth further accelerated
190 during the Yangshao culture period (ca. 7000-5000 BP) and by the late Yangshao culture period (ca.
191 5500-5000 BP), settlements in the region began to display some hierarchical difference. The number
192 of Longshan culture settlements (about 5000-4000 BP) further increased, with the emergence of
193 many walled towns such as the Guchengzhai (Cai and Ma, 2002) and Xinzhai (SACRCPU and
194 ZICH. 2008) walled towns. Whilst the Xia-Shang civilization in the following period (ca. 4000-
195 3000 BP) saw a slight decrease in settlement number compared to the Longshan period, the
196 difference in scale and rank of the Xia-Shang settlements was pronounced. Despite the absence of
197 a capital center, some sites such as Xinzhai (SACRCPU and ZICH. 2008) and Wangjinglou (Gu,

198 2016) were of an enormous scale, and were accompanied with high-rank architecture and artefacts,
 199 indicative of their rank status amongst contemporary sites. This culture sequence in Neolithic and
 200 Bronze-Age Shuangji River valley is similar to that of the Songshan region also on the Central
 201 Plains. Additionally, such a similarity also lies in settlement distribution patterns of the Shuangji
 202 River and Songshan regions. Because prehistoric settlements were concentrated on the loess
 203 tablelands between the low mountains and plains of the Shuangji River valley, we focused in
 204 particular on the loess tablelands in our survey, which covered an area of around 140km² (Figure
 205 1b).



219 Figure 2. Developmental sequences and cultural characteristics of the prehistoric Central Plains and

220 Shuangji River valley. Orange represents the Songshan Mountain region as one of the typical regions
221 with continuous cultural developments on the Central Plains. Blue represents the Shuangji River
222 valley. A. Cultural types and chronologies; B. Settlement numbers. There is a similar growth trend
223 of settlements between the Songshan Mountain region and Shuangji River Basin; C. Farming
224 regimes (Liao et al, 2019). B. Millet = Broomcorn Millet. F. Millet = Foxtail Millet; D. Social
225 complexity and organizational structure as represented by settlement patterns. “Budding Settlement”
226 means there were some signs of long-term habitation, but no houses were found.

227

228 The Palaeolithic populations and the Lijiagou culture in the Shuangji River were subsisted by
229 hunting, gathering and fishing (Qu et al, 2018; Wang C, 2016; Wang YP et al, 2018). Agriculture
230 occurred during the Peiligang culture period when foxtail and broomcorn millets began to be
231 cultivated. Rice remains were also found at some Peiligang culture sites (Wang C, 2017a).
232 Agricultural production remained, however, at a low level during this time, whilst hunting, gathering
233 and fishing were still the main sources of food production (Zhao, 2011). This situation changed
234 drastically during the Yangshao culture period. Dryland farming of foxtail and broomcorn millets
235 became predominant in local subsistence packages and at some sites, the scale of rice farming might
236 have also increased, although it is important to note that hunting, gathering and fishing still
237 contributed significantly to food procurement (Wang C, 2017b). Agriculture further developed
238 during the Longshan culture period, as marked by the introduction of wheat to the region (Deng et
239 al, 2019). In addition to foxtail and broomcorn millets and rice, soybean also began to be cultivated
240 during the Longshan period (Liao et al, 2019). Similarly, gathering, hunting and fishing continued
241 to provide supplementary food to the local populations. By the Xia-Shang period, with the addition

242 of wheat as a crop in the region, the importance of agriculture was further enhanced, although non-
243 agricultural food production still existed (Yao et al, 2007). Overall, subsistence economies in the
244 Neolithic times of the region had been dominated by dryland farming of millets, with the gradual
245 formation of a mixed farming system of rice and millets with later additions of wheat and soybean
246 (Zhang JP et al, 2012; Bestel et al, 2017), whilst gathering, hunting and fishing had been an
247 important supplement to food production. The steady development of prehistoric agriculture in the
248 region benefited from optimal soil and hydrological conditions on stable alluvial and loess
249 landscapes and was foundational to the continuous growth of prehistoric settlements just mentioned.

250 **3. Materials and methods**

251 **3.1 Regional geoarchaeological surveys and sediment lithology analysis**

252 We conducted field surveys in multiple seasons between 2005-2020. These surveys consulted
253 published geological maps (RGSTHGB, 1987) and ascertained general geological and sedimentary
254 characteristics within the Shuangji River region. According to these geological maps, we first
255 divided the area into different geomorphological types. Then the landforms, sedimentary sequences
256 and gully systems at different geomorphological locations were surveyed in greater detail. Based on
257 these works, we drew a regional geomorphological map and schematic vertical and horizontal
258 sections to show topographic variations at the surveyed locations. The regional prehistoric
259 settlements were superimposed on the geomorphological map in order to understand the spatial
260 relationship between the settlement distribution and landform. We also investigated some important
261 and typical archaeological sites during the field surveys. The age, size, distribution of archaeological
262 remains, geomorphological characteristic, sedimentary sequence and hydrologic condition of these
263 sites were recorded.

264 In particular, we examined a series of sedimentary sequences along these river valleys and
265 other alluvial landforms and carefully recorded the sediment logs of these sequences. This
266 information provides direct evidence for regional stratigraphical correlation and reveals intra-
267 regional variation on sedimentary histories that were caused by changes in hydrology and other
268 environmental parameters. Furthermore, this regional stratigraphical correlation also helped to
269 situate the archaeological stratigraphy within their wider geomorphological contexts and therefore
270 understand prehistoric adaptations to diverse landforms and environments in the Shuangji River
271 region.

272 **3.2 OSL and radiocarbon dating**

273 We collected samples for OSL and ¹⁴C dating from sedimentary sequences that are
274 representative of diverse alluvial processes to determine chronologies of them. These sequences
275 have continuous deposition and thus contain rich palaeo-environment information according to our
276 field observation. A total of 51 OSL and nine ¹⁴C dating samples were collected from 12 profiles
277 (Figure 3). OSL dating was completed at the Institute of Geography of Henan Academy of Sciences,
278 whilst ¹⁴C dating was conducted at Peking University and Beta Analytic.

279 The OSL dating adopted the following procedures. 10% mol/HCl was added to the sample to
280 dissolve calcium and carbonate; 30% H₂O₂ was added to remove organic matter. The sediments
281 were then sieved to obtain coarse grained (90–125 μm) and fine (4–11 μm) grained quartz using
282 the method developed and described by Zhang et al. (2010). The purity of quartz was then tested by
283 IR simulation. All measurement was performed on a lexsys research luminescence reader. Single
284 aliquot regeneration (SAR) protocols (Murray and Wintle, 2003) were used to determine the De
285 (equivalent dose) of coarse and fine grained quartz. 25–30 aliquots were measured for each OSL

286 samples. U, TH, and K were measured using neutron-activation-analysis (NAA). The dose rates and
287 OSL ages were determined by the Dose Rate and Age Calculator ('DRAC') (Durcan et al., 2015).

288 Some ¹⁴C dates were obtained from several profiles from a previous study (Lu et al 2019b),
289 which provide a good reference for our present study. The ¹⁴C samples from the SY and NYH
290 profiles were processed by the Accelerator Mass Spectrometer (AMS) at Peking University and Beta
291 Analytic Inc. The AMS ¹⁴C dates were calibrated using the OxCal 4.4.1 software (Ramsey Bronk,
292 1995) and the IntCal 20 calibration curve (Reimer PJ et al, 2020a, 2020b) .

293

294 **3.3 Grain size and soil/sediment micromorphological analyses**

295 Bulk sediment samples were collected from three examined profiles at the PLG, DJ and SY
296 locations (No. 1, 3, 4 in Figure 3a). These profiles are adjacent to the prehistoric settlements and
297 contain characteristic alluvial strata. Samples at the PLG and DJ profiles were collected every 5cm
298 whilst those at the SY profile were collected at an interval of 2cm. A total of 372 bulk samples were
299 collected and analyzed for particle size distribution. The 71 samples from the DJ profile and the 211
300 samples from the SY profiles were processed at the Sedimentary Laboratory of Peking University
301 whilst the 90 samples from the PLG profile were processed at the Institute of Geography of Henan
302 Academy of Sciences, following same procedures described briefly as follows. Diluted HCl and
303 H₂O₂ were added to the samples to remove organic and inorganic carbon, respectively. The sample
304 was then mixed with 10mL 5% sodium hexametaphosphate ((NaPO₃)₆) before being heated on a
305 crucible. This was to fully disperse the particles before they were measured on Malvern Mastersizer
306 2000.

307 Additionally, six soil blocks were collected from the well-preserved and dated palaeosols at

308 the PLG location and made into thin sections. This was completed at the laboratory of the China
309 University of Geosciences (Beijing). The thin sections were examined using polarized microscope
310 following several reference books (Murphy, 1986; Bullock et al, 1985; Stoops, 2003).

311

312 **4. Results**

313 **4.1 Regional geomorphological systems and sedimentary sequences**

314 Through the surveys, we confirmed that regional landform can be divided into two distinctive
315 systems: the Red Clay Hills system and the Pleistocene Alluvial Valley system (Figure 3). As the
316 remnant landform developed from the Tertiary alluvial fans, the Red Clay Hills are presently situated
317 on places with the highest elevation of the region. Controlled by the underlying topography and
318 tectonic activity, the surface of the hill tilts from northwest to southeast, ranging in altitude between
319 130-300 m. The stratum on the Red Clay Hills is dominated by Tertiary sediments including gravels
320 and clay. Overlying the Tertiary sediments are thin layers of Pleistocene loess. Whilst some
321 Neolithic and Bronze Age settlements were located on the red-clay landforms, these accounted for
322 a small number compared to those settlements located on the alluvial valleys.

323 The Pleistocene alluvial valleys are mainly distributed on both sides of the Shuangji River and
324 along its largest tributary, the Zhenshui River basin. The geomorphological system consists of, in
325 particular, four-ordered river terraces in the valleys. Alluvial terraces T4 are the highest terraces in
326 the region and their elevation is almost the same as the red clay hills. The surfaces of the terraces
327 are generally more than 35 meters above the valley bottom. The terrace sediments are mainly of
328 loose Quaternary sediment clasts. Overall, the distribution of alluvial terraces T4 is scattered, only
329 present at a few locations such as near the Peiligang site (Figure 4). In contrast, alluvial terraces T3

330 are widely distributed in the Shuangji River and Zhenshui River valleys. The surfaces of them are
331 flat and wide, ca. 20-25 m higher than the valley bottoms. The sediments are dominated by Late
332 Pleistocene and Holocene aeolian loess, but thick layers of Late Pleistocene fluvio-lacustrine
333 sediments with embedded channel deposits can be seen in many examined profiles such as the DTQ
334 and PLGXG sections during our surveys. Many Neolithic-Bronze settlements were densely
335 distributed on top of the alluvial terraces T3, including the large-scale sites at Xinzhai and
336 Guchengzhai. Alluvial terraces T2 are less well-preserved along the main channels of the Shuangji
337 River and Zhenshui River due to river erosion. But a few alluvial terraces T2 are preserved along
338 some small valleys. The surfaces of some alluvial terraces T2 are almost as flat and wide as those
339 of the alluvial terraces T3. The age of alluvial terraces T1 is relatively young, of the late historical
340 period. These terraces are narrower and generally distributed on both sides of the Shuangji River,
341 Zhenshui River and their tributaries.

342 Because the Neolithic and Bronze-Age settlements were mostly distributed on the alluvial
343 terraces T3 and T4, we paid more attention to these terraces and surrounding landforms along the
344 Shuangji River and its tributaries such as the Zhenshui River. Through the geomorphological and
345 geoarchaeological surveys, we established spatial and temporal variations of alluvial landforms
346 along these rivers and their relationships with prehistoric settlements.

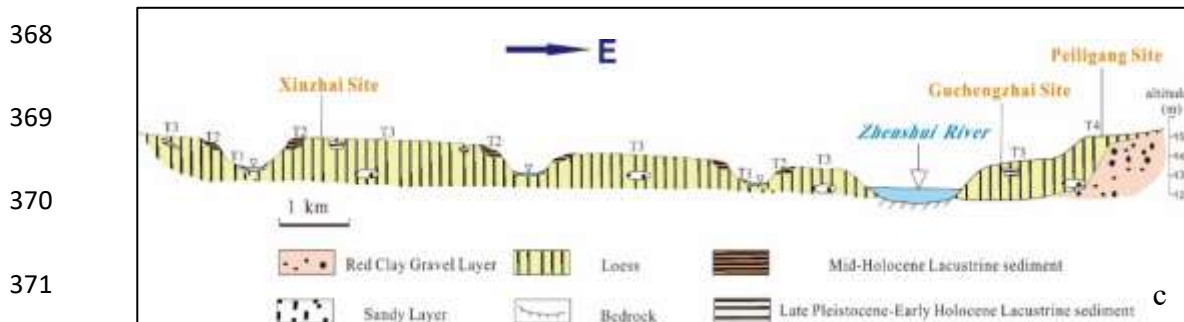
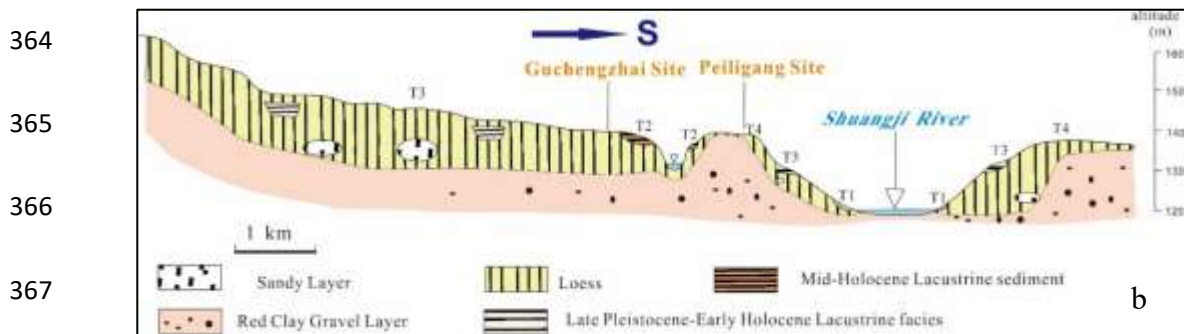
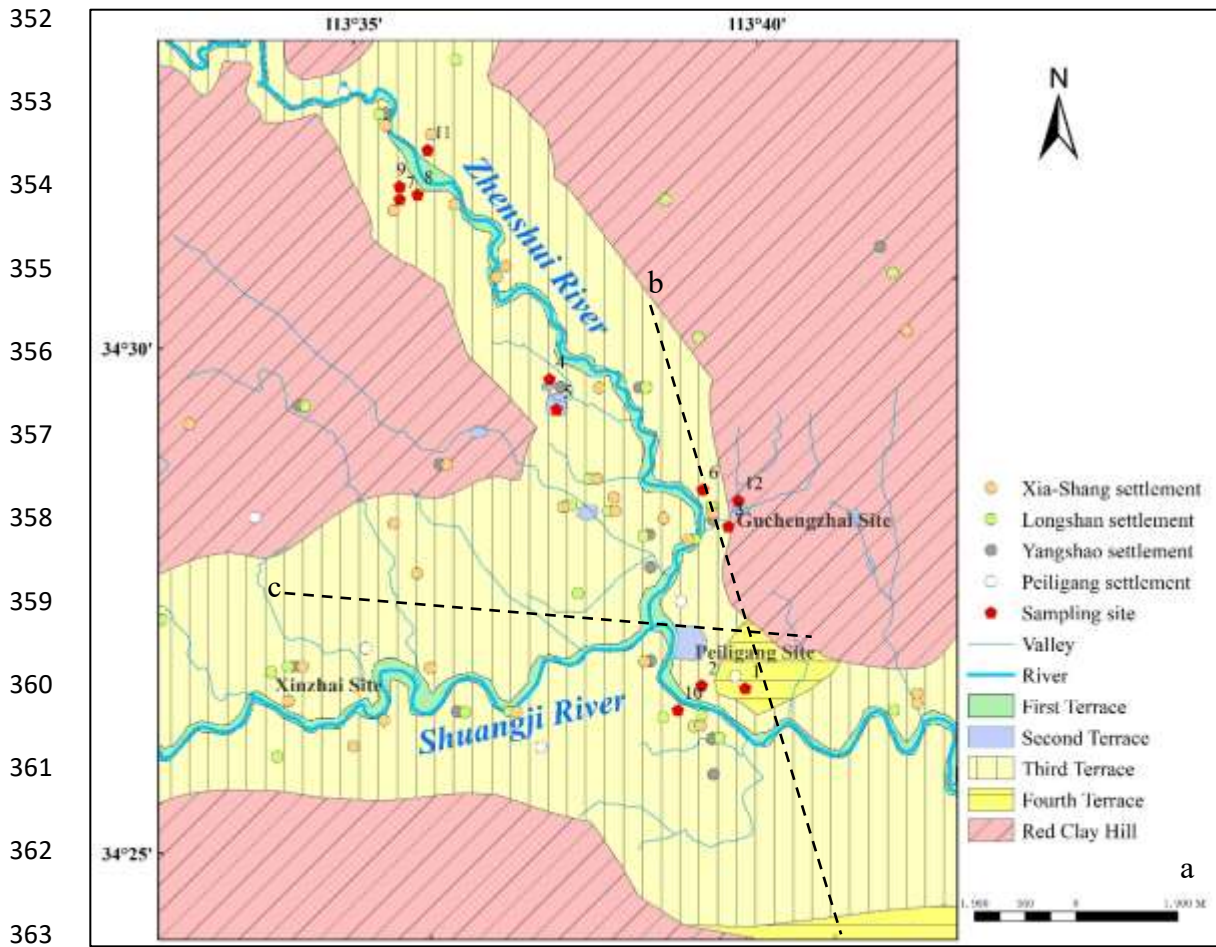
347

348

349

350

351



372 Figure 3. Regional geomorphology and distributions of Neolithic and Bronze-Age settlements. a.

373 The geomorphological types and settlement distributions. The red pentagons indicate the locations

374 of the stratigraphic sections examined in this paper. 1: PLG. 2. PLGXG. 3. DJ. 4. SY. 5. NYH. 6.
 375 GCZ. 7. MSQ. 8. QLN 1. 9. QLN 2. 10. DTQ. 11. QL. 12. XHZ; b. Schematic south-north cross
 376 section of the studied region. The locations are marked in Figure 3a; c. Schematic west-east cross
 377 section. The locations are marked in Figure 3a.



394 Figure 4. Satellite image of the Shuangji River valley. a. The satellite image shows that there
 395 are four-ordered alluvial terraces in the Shuangji River valley near the Peiligang Site. The vertical

396 distance between the surfaces of alluvial terraces T4, T3, T2 and T1 to the river are about 35m, 25m,
397 15m and 5m, respectively (The data is collected from MAPWORLD); b. Stratigraphy from the
398 excavation at the Peiligang site situated on top of alluvial terrace T4. The top is the cultural layer
399 containing Peiligang Culture (8000 a BP) and Erligang Culture (3500 a BP) remains, note the
400 significant cultural hiatus at the site. The second layer is the Holocene palaeosol. The third layer is
401 the local sheet flow sediments. The bottom is the late Pleistocene loess; c. The alluvial deposits date
402 to the terminal Pleistocene and early Holocene at alluvial terrace T3 from the DW Section, 1km
403 north of the Peiligang site; d. The middle Holocene alluvium on alluvial terrace T2 from the SY
404 Section).

405

406

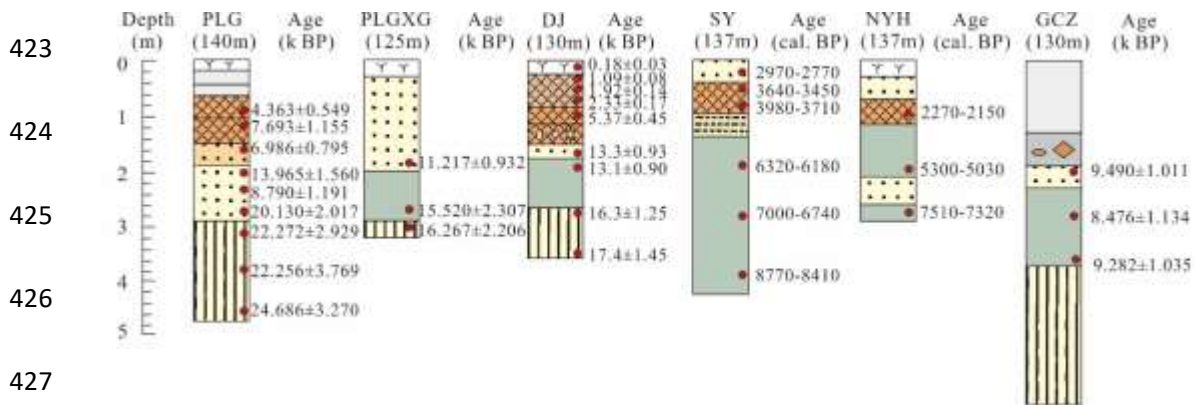
407 Amongst all the examined stratigraphies, only the PLG section is located on alluvial terraces
408 T4 ([Figure 4, 5. Stratigraphic description see the supplementary information document](#)). As shown
409 in the figure, the section is dominated by loess-palaeosol deposits. Whilst alluvial deposits were
410 present at the PLG section, they were only a local phenomenon, such alluvial deposits rarely occur
411 in other excavation trenches at the site. In other words, the local landscape remained stable and was
412 rarely affected by alluvial processes during the Late Pleistocene and early Holocene.

413 Seven of our examined profiles, including PLGXG, DJ, GCZ, MSQ, QLN2, DTQ, QL (No. 2,
414 3, 6, 7, 9, 10, 11 in Figure 3a) belong to alluvial terraces T3 ([Figures 4 and 5](#)). These sections
415 generally contain some alluvial strata which are mostly of lacustrine facies that were deposited
416 during the terminal Pleistocene to the early Holocene.

417 The SY, NYH, QLN1, XHZ sections (No. 4, 5, 8, 12 in Figure 3a) are all distributed along the

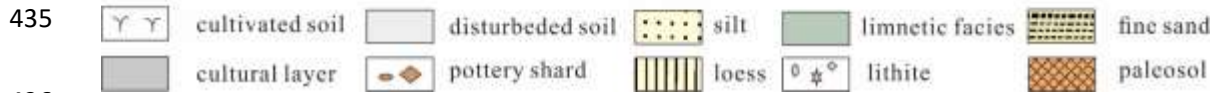
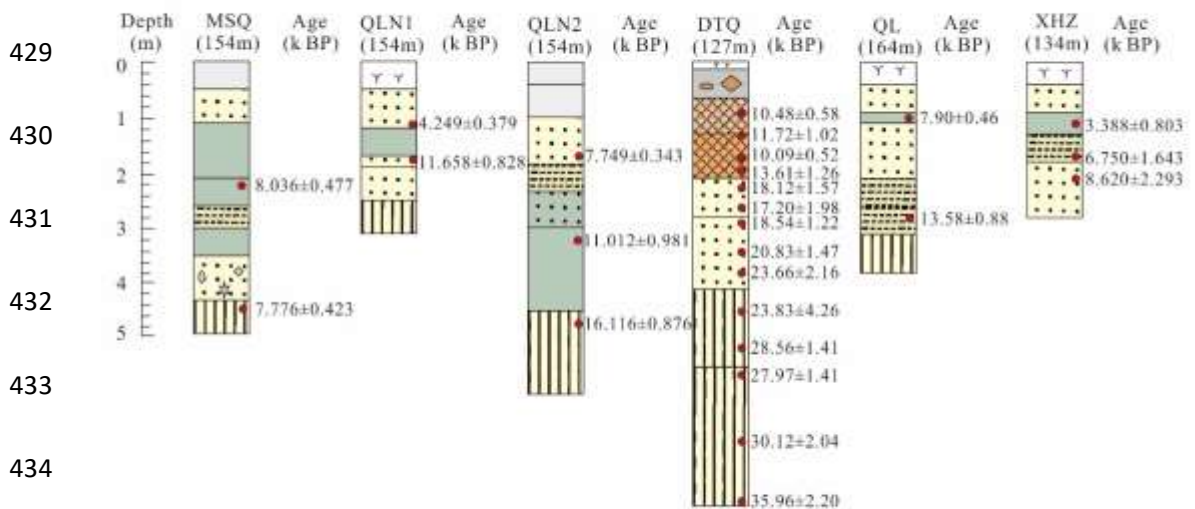
418 tributary gullies of the rivers in the region. The presence of lacustrine sediments in some of the
 419 profiles also points to high regional water table which was probably induced by climate change. We
 420 can also infer that these sections should be parts of the alluvial terraces T2 which formed on tributary
 421 gullies during the middle Holocene.

422



426

427



436

437 Figure 5. Sediment logs of examined stratigraphic profiles. The positions of sections are shown in

438 figure 3a. The top elevation of every section has been labeled on the stratigraphic diagram. The

439 dates in SY and NYH profiles are AMS ¹⁴C ages which have been published in Lu et al (2019).

440 4.2 Chronological framework of the alluvial landform evolution

441 The results of OSL dates are summarized in [Table 1](#). The preheating test shows that both the 220 °C
442 for coarse-sized samples (90-125 μ m) and the 240 °C for fine-sized samples (4-11 μ m) are
443 appropriate preheating temperatures ([Figure 6](#)). The over-dispersion rate of most samples is less
444 than 15% which indicates that the effective dose results of the test are relatively concentrated ([Table](#)
445 [1](#)). Some De values with larger over-dispersion rate such as samples no. MSQ03, QLN1-01 and
446 QLN1-02 are reprocessed using the chronological model. The recycling ratio of most samples is
447 between 0.9-1.1 which indicates that the correction of sense sensitive quality change is successful.
448 The recuperations are within 5% which is an acceptable range. OSL decay curves show that the
449 samples have been bleached well. All the above qualities ensure the reliability of the OSL results.
450 Most OSL dates fall into good chronological orders and were consistent with our field estimation of
451 the dates of the stratigraphies except for a few anomalies. Because of the possible incomplete light
452 bleaching or sample exposure, sample no. PLG005 from the PLG site was abnormally young and
453 was therefore not considered here. Similarly, sample no. DTQ1-4 was significantly older than the
454 estimated age. Importantly, although date reverses occurred at the GCZ, MSQ and DTQ profiles,
455 they were within the range of standard deviation and were thus considered alongside field
456 observations to establish chronologies of the sedimentation histories at these locations.

457

458

459

460

461

Table 1. The results of OSL dating

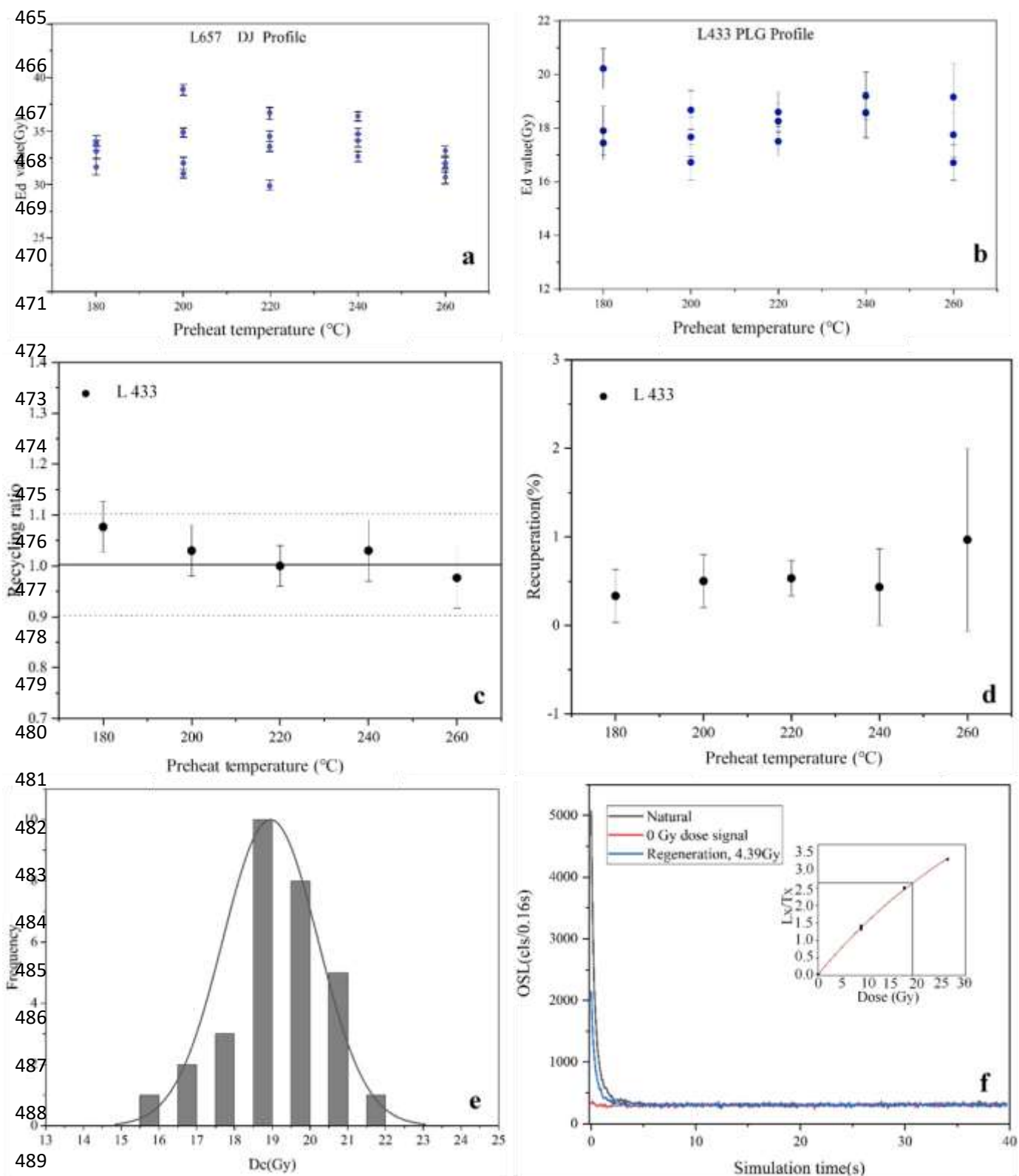
462

463

Sample No.	Lab. No	Depth(cm)	U/ppm	Th/ppm	K/%	Rb/ppm	Q-De(Gy)	OD(%)	w.c (%)	Q-Dose rate	Q-Age(ka)
PLG 001	L433	80	2.58±1.92	15.3±1.29	2.07±0.44	101±1.62	18.55±0.30	5.13	10.58	4.252±0.530	4.363±0.549
PLG 002	L434	115	2.30±2.37	13.4±1.47	2.03±0.43	102±1.18	30.04±0.92	8.65	11.68	3.905±0.574	7.693±1.155
PLG 003	L435	160	2.35±1.49	13.7±1.20	2.01±0.38	97.7±1.51	27.45±0.67	7.74	11.35	3.929±0.437	6.986±0.795
PLG 004	L436	200	2.17±1.34	11.2±2.22	1.96±0.34	90.6±1.32	51.47±1.38	8.49	9.16	3.686±0.400	13.965±1.560
PLG 005	L437	245	2.26±0.74	13.9±0.95	2.02±0.62	93.4±1.05	35.20±1.19	8.94	9.13	4.005±0.525	8.790±1.191
PLG 006	L438	290	2.10±1.29	11.8±1.19	2.00±0.28	92.5±1.89	73.98±1.64	5.96	10.70	3.675±0.359	20.130±2.017
PLG 007	L439	335	2.24±1.31	12.8±0.42	1.87±0.50	86.5±0.75	81.07±1.98	6.59	11.61	3.640±0.470	22.272±2.929
PLG 008	L440	380	2.22±2.75	11.1±1.05	1.87±0.35	86.0±1.67	76.75±0.75	2.66	12.43	3.448±0.583	22.256±3.769
PLG 009	L441	460	2.07±1.86	12.8±1.28	1.78±0.35	80.9±0.79	85.50±0.74	2.20	12.22	3.464±0.458	24.686±3.270
PLGXG 001	L442	200	2.13±1.34	14.5±0.99	2.23±0.20	118±0.24	45.45±0.27	1.91	13.18	4.052±0.336	11.217±0.932
PLGXG 002	L443	245	1.94±1.19	13.2±0.75	2.05±0.66	105±0.84	57.10±0.38	2.10	13.92	3.679±0.546	15.520±2.307
PLGXG 003	L444	290	1.75±1.94	11.2±1.06	1.90±0.33	86.3±0.99	56.73±0.43	2.40	8.91	3.487±0.472	16.267±2.206
DJ001	PKU L652	8±3	3.71±0.45	10.77±1.49	1.75±0.1		0.55±0.07	12.73	20±5	3.1±0.2	0.18±0.03
DJ002	PKU L653	23±3	2.38±0.40	11.95±1.35	1.75±0.1		3.08±0.11	9.74	20±5	2.8±0.2	1.09±0.08
DJ003	PKU L654	43±3	2.95±0.43	11.16±1.43	1.78±0.1		5.55±0.21	9.01	20±5	2.9±0.2	1.92±0.14

DJ004	PKU L655	63±3	2.96±0.43	11.04±1.43	1.62±0.1		6.40±0.13	7.81	20±5	2.8±0.2	2.33±0.17
DJ005	PKU L656	95±5	2.84±0.46	12.65±1.53	1.60±0.1		15.04±0.63	4.19	20±5	2.8±0.2	5.37±0.45
DJ006	PKU L657	170±5	3.16±0.37	9.23±1.22	1.50±0.1		33.99±0.34	1.47	20±5	2.6±0.2	13.3±0.93
DJ007	PKU L658	185±5	2.70±0.37	9.63±1.22	1.70±0.1		34.60±0.44	1.45	20±5	2.6±0.2	13.1±0.90
DJ008	PKU L659	268±3	2.92±0.44	11.14±1.47	1.55±0.1		43.17±1.09	2.52	20±5	2.6±0.2	16.3±1.25
DJ009	PKU L660	353±3	3.78±0.40	8.30±1.33	1.70±0.1		47.90±2.25	4.70	20±5	2.8±0.2	17.4±1.45
GCZ001	L425	200	2.05±1.20	13.0±1.75	1.72±0.27	96.4±1.65	36.48±1.17	8.51	3.06	3.844±0.391	9.490±1.011
GCZ002	L426	280	1.99±1.65	13.6±0.43	1.84±0.44	115±1.60	32.83±0.87	7.47	5.64	3.873±0.508	8.476±1.134
GCZ003	L427	370	2.15±1.22	11.8±0.92	1.65±0.32	85.4±1.62	33.29±0.67	6.32	4.65	3.586±0.393	9.282±1.035
MSQ01	L046	450	2.23±4.1	10.3±2.8	1.66±3.3		30.26±0.83	4.92	6.03	3.415±0.161	7.776±0.423
MSQ02	L047	220	1.97±4.2	9.65±2.9	1.67±3.3		32.32±1.18	11.91	1.35	3.310±0.149	8.038±0.477
MSQ03	L048	180	1.97±4.2	9.06±2.9	1.61±3.3		34.07±1.92	16.59	28.20	3.216±0.144	11.658±0.828
QLN1-01	L049	110	2.05±4.2	9.38±2.9	1.83±3.1		16.4±1.05	20.18	1.61	3.387±0.153	4.249±0.379
QLN1-02	L050	470	1.89±4.3	7.49±3.2	1.78±3.2		60.27±2.10	31.47	3.20	3.874±0.178	16.116±0.876
QLN2-01	L051	320	2.56±3.9	12.1±2.8	1.80±3.1		41.00±4.18	11.75	2.80	3.750±0.174	11.012±0.981
QLN2-02	L052	170	1.86±4.4	8.79±3.0	1.64±3.3		29.34±0.30	3.06	3.9	3.442±0.155	7.749±0.343
DTQ01	20150101	95	2.15±4.1	10.3±2.8	1.99±3.0	93.8±5.4	36.97±1.49	4.17	10±5	3.55±0.14	10.41±0.58
DTQ02	20150102	130	2.08±4.2	10.3±2.8	1.77±3.2	92.9±5.7	38.90±3.04	10.06	10±5	3.32±0.13	11.72±1.02
DTQ03	20150103	170	2.17±4.1	11.0±2.8	1.84±3.1	88.4±6.0	34.92±1.21	8.72	10±5	3.46±0.13	10.09±0.52
DTQ04	20150104	200	2.05±4.2	9.91±2.8	1.88±3.1	90.4±5.8	45.76±3.87	5.34	10±5	3.36±0.13	13.61±1.26

DTQ05	20150105	230	1.95±4.3	10.1±2.8	1.90±3.0	87.4±6.1	60.88±4.72	9.15	10±5	3.36±0.13	18.12±1.57
DTQ06	20150106	260	1.95±4.3	10.7±2.8	2.04±3.0	90.6±5.8	60.77±6.60	10.23	10±5	3.53±0.14	17.20±1.98
DTQ07	20150107	290	2.22±4.1	10.1±2.8	1.92±3.0	95.3±5.6	63.97±3.43	4.33	10±5	3.45±0.13	18.54±1.22
DTQ08	20150108	340	2.10±4.2	10.5±2.8	1.96±3.0	87.0±6.1	72.34±4.29	7.06	10±5	3.47±0.13	20.83±1.47
DTQ09	20150109	380	2.26±4.1	9.88±2.8	1.95±3.0	82.5±6.3	81.63±6.76	8.72	10±5	3.45±0.13	23.66±2.16
DTQ10	20150110	450	2.13±4.2	10.5±2.8	1.80±3.1	88.3±6.1	79.10±13.82	6.69	10±5	3.32±0.13	23.83±4.26
DTQ11	20150111	520	1.59±4.7	8.54±3.0	1.80±3.1	85.5±6.1	85.16±2.55	10.27	10±5	2.98±0.12	28.56±1.41
DTQ12	20150112	570	1.58±4.7	8.61±3.0	1.65±3.3	83.8±6.2	79.47±2.55	7.78	10±5	2.84±0.11	27.97±1.41
DTQ13	NJU2050	690	1.76±0.08	8.48±0.25	1.55±0.05		77.36±2.56	10.99	7.16±5	2.57±0.14	30.12±2.04
DTQ15	NJU2051	800	1.78±0.08	8.21±0.25	1.48±0.05		88.44±1.44	6.98	7.8±5	2.46±0.14	35.96±2.20
DTQ19	NJU2052	1100	1.70±0.08	8.90±0.26	1.72±0.06		106.83±1.33	4.30	6.81±5	2.73±0.16	39.10±2.41
DTQ24	NJU2053	1350	1.61±0.08	7.61±0.24	1.50±0.05		83.42±1.11	4.62	7.3±5	2.38±0.13	34.98±2.51
DTQ26	NJU2054	1590	2.23±0.09	9.10±0.26	1.54±0.05		115.88±3.10	12.25	7.06±5	2.65±0.15	43.77±2.88
QL01	L 080	100	1.81±0.08	10.3±0.29	1.55±0.05	77.50±4.65	24.47±0.30	2.96	10±5	3.10±0.18	7.76±0.46
QL02	L 081	280	1.74±0.08	7.43±0.24	1.32±0.05	62.80±4.52	34.79±1.09	7.67	10±5	2.56±0.15	13.58±0.88
XHZ 01	L495	110	2.08±4.0	11.4±3.2	1.67±0.13	85.3±2.3	12.60±0.10	2.62	1.95	3.719±0.881	3.388±0.803
XHZ 02	L496	172	2.06±1.7	10.5±2.2	1.50±0.88	86.8±2.7	22.86±0.10	1.44	3.11	3.387±0.824	6.750±1.643
XHZ 03	L497	205	1.93±2.1	10.8±2.7	1.60±0.96	80.4±1.8	30.29±0.23	2.39	1.87	3.514±0.934	8.620±2.293



490 Figure 6. Graphs showing OSL dating procedures. a. Preheating test for sample no. L660 of the DJ
 491 profile shows that 220 °C is an appropriate preheating temperature for coarse-sized samples (90-
 492 125 μ m); b. Preheating test for sample no. L433 of PLG profile shows that 240 °C is an
 493 appropriate preheating temperature for fine-sized samples (4-11 μ m); c. Recycling ratio of the

494 sample no. L433 of PLG profile; d. Recuperation of the sample no. L433 of PLG profile; e. The
495 recycling ratio histogram for all measured aliquots of sample no. L433; f. The decay curves and
496 growth curve for sample no. L433.

497

498

499 Our ¹⁴C dating results ([Table 2](#)) accord well with the OSL dates. Both the SY and NYH profiles are
500 located on alluvial terraces T2 along tributary gullies, with similar sedimentary sequences ([Lu et al,](#)
501 [2019b](#)). The ages of the alluvial sediment in these sections fall between 4000-8000 a BP (Table 3).
502 The OSL results provide the sedimentation ages of the other two terraces at XHZ and QLN1. The
503 alluvial sediments of these sections also fall between 8000-4000 a BP. These indicate that the
504 tributary gullies were at an accretion state during 8000-4000 a BP. After 4000 a BP, the regional
505 river system began a downcutting process which led to the formation of alluvial terraces T2.
506 Unfortunately, there are few alluvial terraces T2 preserved on either side of the main rivers such as
507 the Shuangji River and Zhenshui River in the region. Rather, they are found in scattered distribution
508 along the tributary gullies.

509

510

511

512

513

514

515

516

517

518

519

520

521

522

523

Table 2 The results of radiocarbon dating (Lu et al, 2019b)

524

Sample Code	Sampling Site	Lab codes	Texture	Dating materials	Depth (cm)	¹⁴ C age (BP)	Calibrated age cal BP(2σ)
SY205	Shiyuan	BA07087	loess	organic sediment	12-14	2775±40	2970 - 2770
SY189	Shiyuan	BA07086	paleosol	organic sediment	44-46	3330±40	3650 - 3160
SY177	Shiyuan	BA07085	sand	organic sediment	104-106	3560±40	3980 - 3720
SY117	Shiyuan	BA07083	limnetic facies	organic sediment	188-190	5455±40	6320 - 6180
SY74	Shiyuan	BA07081	limnetic facies	organic sediment	274-276	6045±45	7010 - 6750
SY18	Shiyuan	BA07079	limnetic facies	organic sediment	386-388	7800±60	8770 - 8420
NYH003	Niuyuhuan	Beta- 25589	paleosol	organic sediment	90	2120±30	2345-2295 2270-2155
NYH002	Niuyuhuan	Beta-425588	limnetic facies	organic sediment	195	4350±30	5300-5035 5005-4980
NYH001	Niuyuhuan	Beta-425587	limnetic facies	organic sediment	275	6380±40	7480-7415 7390-7370 7355-7330

525

526 Most OSL ages of the alluvial sediments on terraces T3 are largely concentrated between
527 13000- 8000 BP (Table 3). Despite the age of PLGXG is a little old, it is still within the margin of
528 error. The Depth-Age Model of the DJ profile shows that the lacustrine deposits at 270-180 cm deep
529 also have an age of between 13000-8000 BP (Figure 7). The presence of lacustrine deposits suggests
530 it was a river aggradation process during the time. After 8000 BP, the regional rivers began to incise
531 the landscape. This was followed by a stage of landscape stability which formed the loess-paleosol
532 sequences on the terraces.

533

Table 3 Summary of the age of alluvial deposits in terraces T3 and T2

Geomorphic position	Profile	Sedimentary facies	Age (ka BP)
Alluvial terraces T3	PLGXG	Lacustrine facies	15.520 ± 3.207
	DJ	Lacustrine facies	13.1 ± 0.9
	GCZ	Lacustrine facies	$8.476 \pm 1.134 - 9.282 \pm 1.035$
	MSQ	Lacustrine facies	8.036 ± 0.477
	QLN2	Lacustrine facies	11.012 ± 0.981
	QL	Lacustrine facies	7.90 ± 0.46
Alluvial terraces T2	SY	Lacustrine facies, Fluvial faces	$8.770 - 3.980$
	NYH	Lacustrine facies	$7.510 - 5.030$
	QLN1	Lacustrine facies	4.249 ± 0.379
	XHZ	Lacustrine facies, Fluvial faces	$3.388 \pm 0.803 - 6.750 \pm 1.643$

535

536

537 The Depth-Age Model of the PLG profile shows that the alluvial terraces T4 enjoyed a
538 relatively stable hydrological environment since 14000 a BP during which soil sequences developed
539 whilst loess continued to accumulate as evidenced by the presence of typical loess-palaeosol
540 sequence. The field survey and laboratory sediment analysis showed that there were some older age
541 (18000-14000 a BP) sheet flow deposits in the PLG profile, but with an overall limited distribution.
542 We estimate the terraces formed before 30,000 a BP according of the OSL date of the sample
543 collected from the bottom of PLG section (Figure 7b).

544

545

546

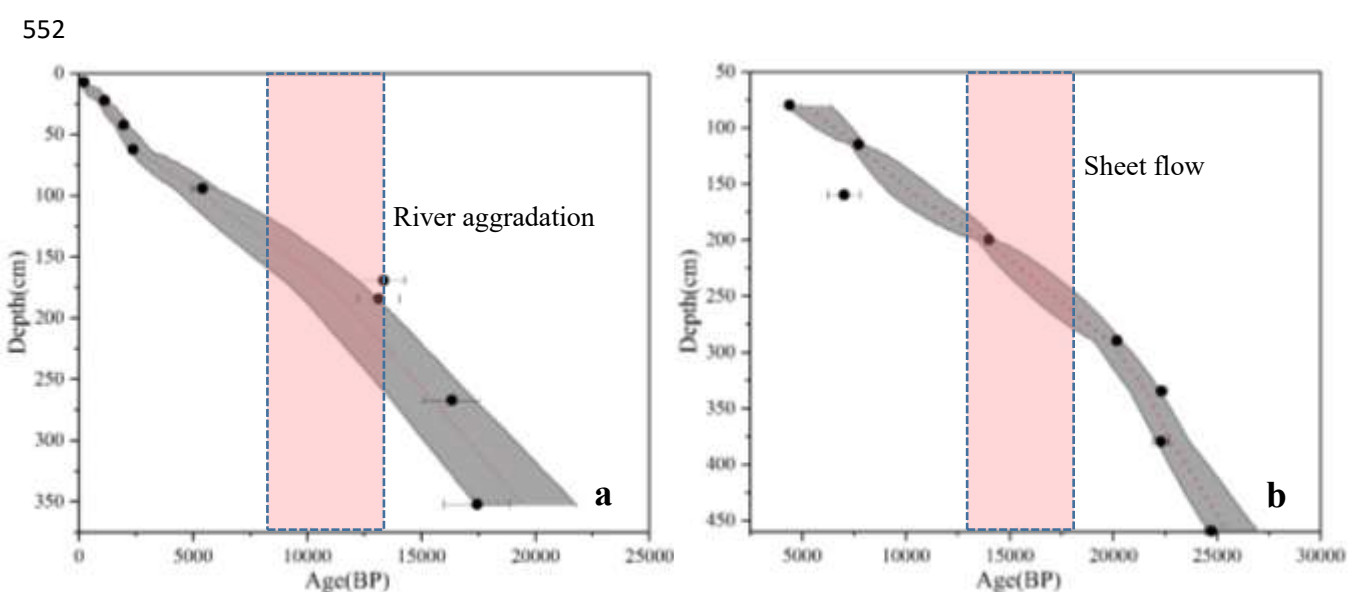
547

548

549

550

551



562 Figure 7. Depth-Age Model. a. The DJ profile shows an episode of river aggradation between
 563 13000-8000 BP (red part); b. The PLG profile shows a local sheet flow 18000-14000 BP (red part);

564

565 **4.3 Reconstructing late-Pleistocene and Holocene sedimentation histories: particle size and**
 566 **soil micromorphology of the PLG and DJ profiles**

567

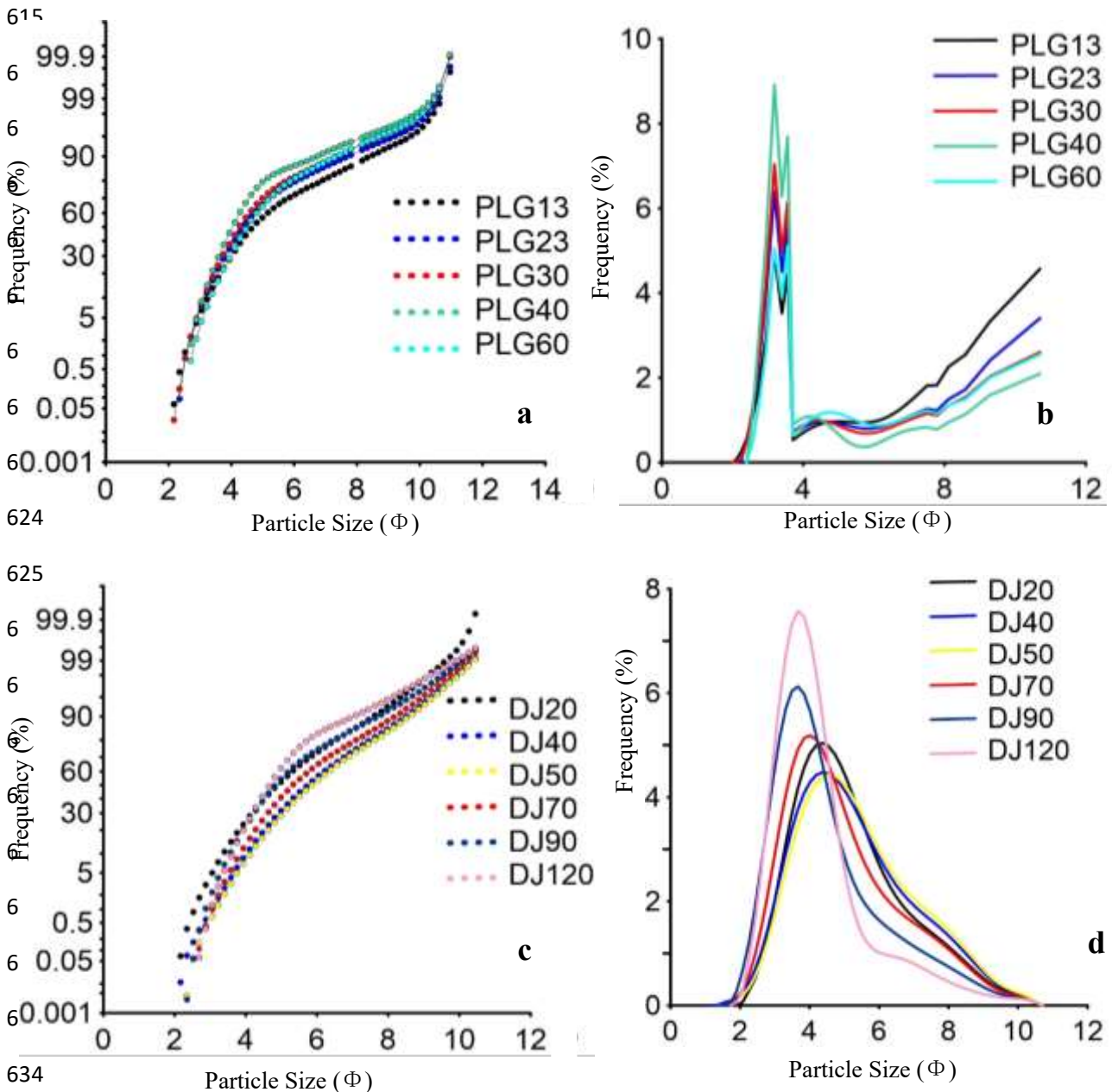
568 Results of the selected sediment samples from the PLG and DJ profiles that were analyzed for
 569 particle size distribution are presented in Figure 8. The frequency cumulative curves of sample no.
 570 PLG-60 show that saltation particles smaller than 4ϕ account for 10%, whilst the suspended load
 571 particles larger than 4ϕ were more than 70%. Other particles fall into the intermediate size range.
 572 Overall, such a distribution pattern indicates that the sediments were of typical wind-blown loess
 573 being deposited during the late Pleistocene. Micromorphological features of the soil thin section
 574 collected from the same layer (Layer 8; Figure 9) at the site further confirm the poor-sorting and
 575 coarse-size nature of the wind-blown sediments that came from a nearby source. The presence of
 576 abundant calcitic features in the thin section suggest a relatively dry condition during the time. For
 577 the frequency cumulative curves of samples nos. PLG-40, PLG-30, and PLG-23, particles smaller
 578 than 4ϕ account for 70%. The remaining 30% are suspending particles. The distribution of two
 579 narrow peaks on their frequency curves points to a good sorting of the sediments under strong
 580 hydrodynamic conditions. These results illustrate that layers 5, 6, and 7 in the PLG profile represent

581 a sedimentation environment resembling that of a point bar and floodplain. Soil thin sections from
582 these layers (PLG005, PLG004 and PLG003) reveal similar scenarios of sedimentation and post-
583 depositional processes. The groundmass of thin section no. PLG005 is characterized by rounded-
584 shaped minerals and the significantly reduced calcite in the groundmass, whilst the presence of some
585 thin clay coatings indicates incipient soil formation. The sediments gradually became more poorly
586 sorted from PLG004 to PLG003, but with increased pedofeatures indicative of soil formation. These
587 results suggest that, interestingly, whilst the sedimentation environment on the alluvial settings
588 continued to be volatile, there was increasing disturbance on the surface, as evidenced by the
589 presence of dusty clay coatings, which was probably caused by human or related cultural activities
590 (Figures 9b and 9c). Comparatively speaking, the percentage of particles smaller than 4ϕ accounted
591 for ca.10% as shown by the frequency cumulative curves of sample no. PLG-13, whilst the
592 frequency curves suggest that the sediments were overall poorly sorted (Figure 8). Furthermore, the
593 significant proportion of clay-sized particles also indicates strong degree of soil formation during
594 the middle Holocene. The latter was accompanied with intensified human activities as evidenced by
595 the micromorphological features of abundant charcoal and clay textural features in thin section no.
596 PLG002 (Figure 9d).

597 Amongst the examined samples from the DJ profile, samples nos. DJ-90 and DJ-120 contained
598 ca.70% of bedload-movement and saltation particles. Given their narrow-peaked distribution, they
599 represent well-sorted lacustrine sediments deposited during the late phase of the late Pleistocene.
600 The light grayish colour of the sediments also suggests post-depositional gleying and redoxmorphic
601 processes. The other four samples (nos. DJ-20, DJ-40, DJ-50 and DJ-70) contained only 10% of
602 saltation particles, in contrast to 90% of suspended load sediments. The sediments are poorly sorted
603 with increasing percentage of coarse-sized particles. The concentration of fine-sized particles in
604 sample no. DJ-50 indicates strong degree of soil formation before chemical weathering became
605 weaker again in the profile as suggested by the decreasing percentage of clay in the sediments
606 (Figure 8).

607 These results are consistent with published studies which confirm that the sediment source for
608 late Pleistocene and Holocene loess in the eastern Songshan region mainly came from the Yellow
609 River floodplain situated to the east of the Mengjin section of the river (Jiang et al, 1997; Yang YM

610 et al, 2005; Pang et al, 2008). Its size gradually decreased eastwards as wind blowing activities
 611 became more distant from the source area. Comparing with other published similar studies in the
 612 adjacent areas (Lu et al, 2021; Xu et al, 2013) our results of particle size distribution of samples
 613 from the PLG and DJ profiles show that the late Pleistocene and Holocene sediments are dominated
 614 by silt-sized particles of loess or reworked loess.



635 Figure 8. Particle size distribution for the PLG and DJ profiles. a. Cumulative probability curves of
 636 the PLG profile; b. Frequency distribution curves of the PLG profile. c. Cumulative probability
 637 curves of the DJ profile; d. Frequency distribution curves of the DJ profile. According to the results,
 638 samples no. PLG-23, PLG-30 and PLG-40 should represent fluvial facies, whilst samples no. XD-

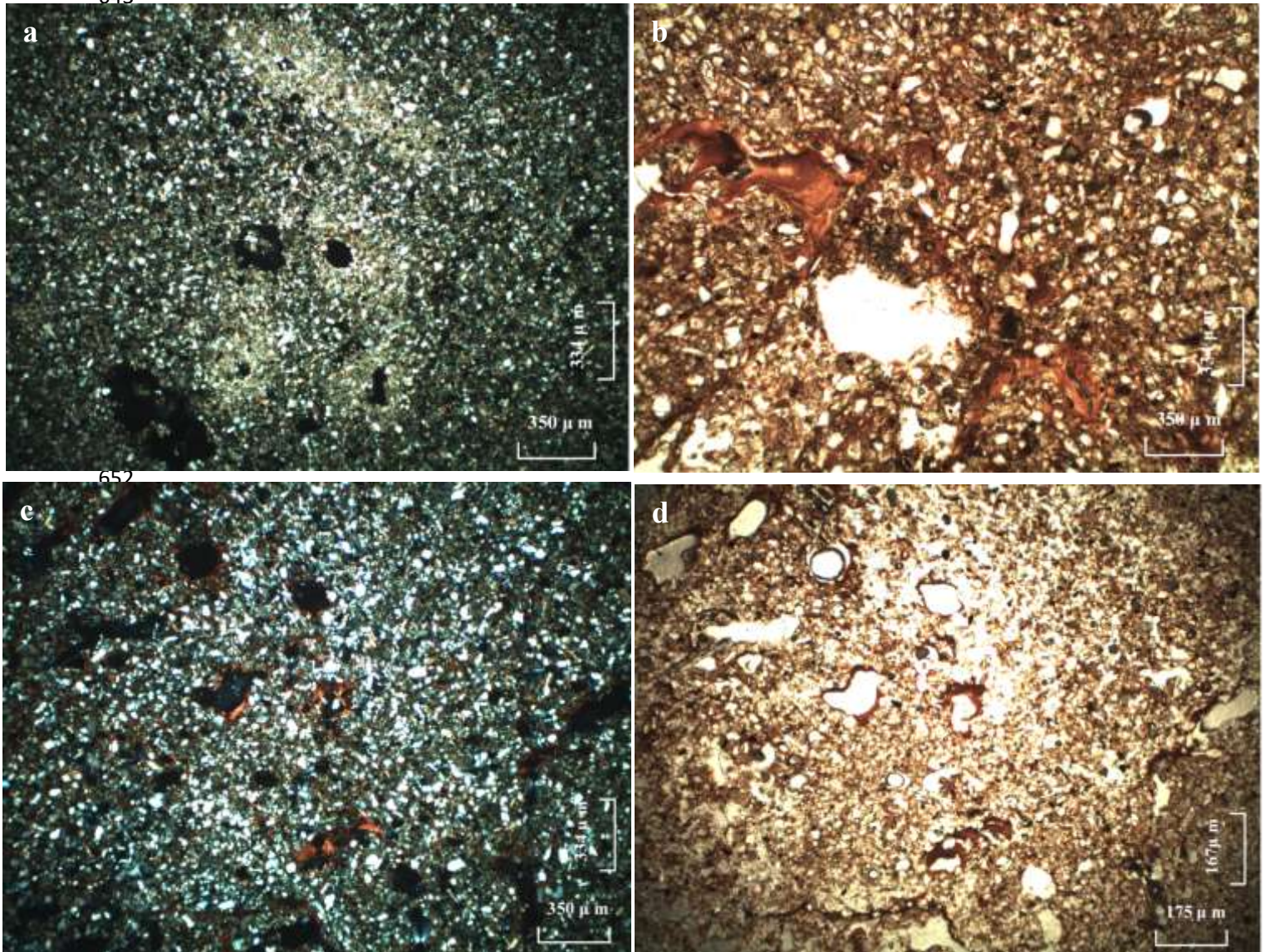
639 90、XD-120 should represent limnetic facies. The others are all loess deposits.

640

641

642

643



662 Figure 9 Microphotographs of thin section slides from the PLG profile. a. sample no. PLG006,

663 calcitic nodules and coatings and hypo-coatings. Note that well-sorted wind-blown very fine sand-

664 sized sand and silt in the groundmass, containing abundant quartz and micas; b and c. sample no.

665 PLG004, clay coatings with layered structure and modest birefringence, PPL and XPL; d: sample

666 no. PLG002-bottom, clay textural features with layered structure in micro-charcoal and organic rich

667 groundmass. PPL.

668 **5. Discussion**

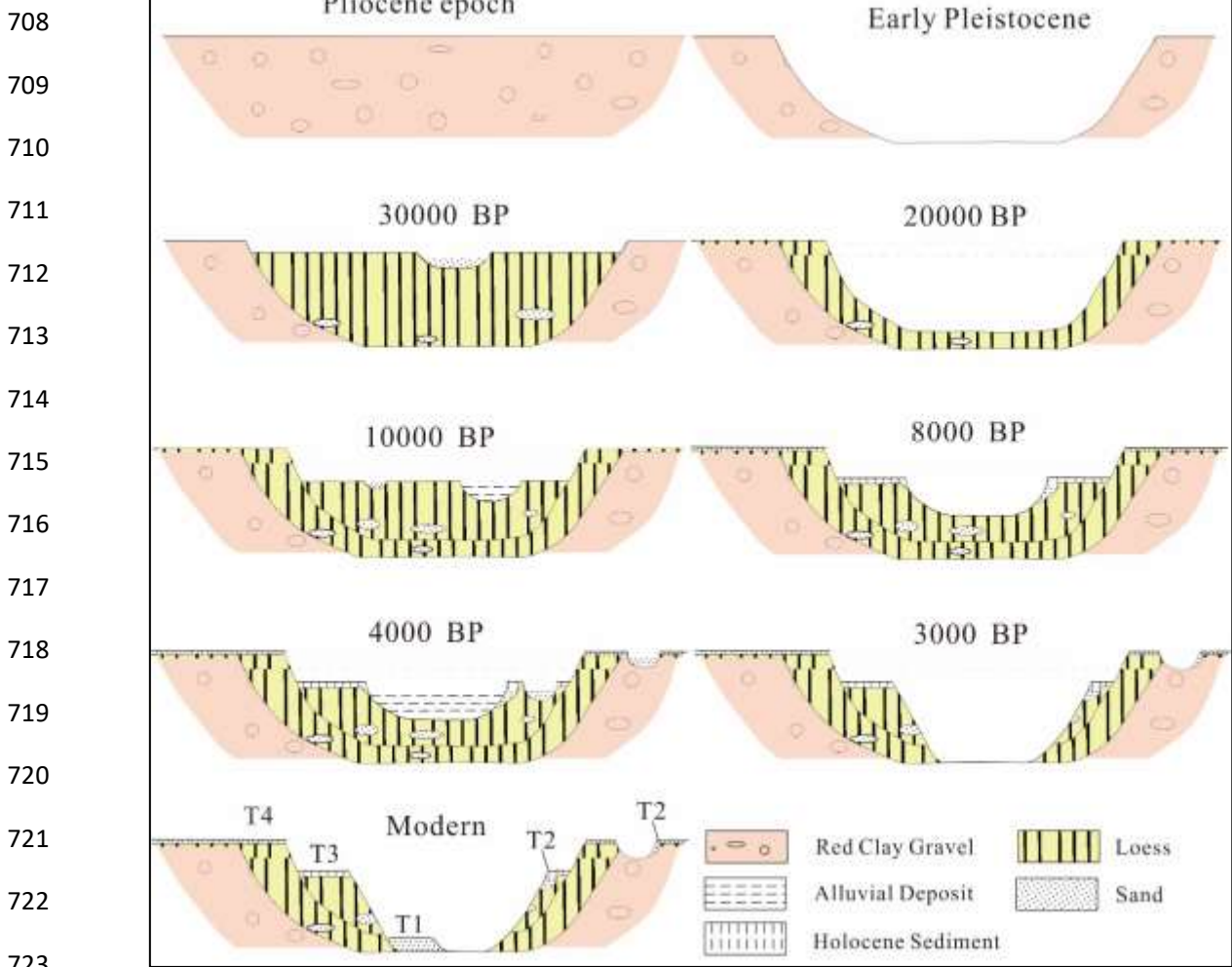
669 **5.1 Evolution of late Pleistocene to Holocene alluvial landscapes**

670 Combining field survey data, chronological data, and results of particle size and
671 micromorphological analyses, we were able to reconstruct evolution of late Pleistocene to Holocene
672 alluvial landscapes in the Shuangji River region. Our data suggest that Tertiary red clay landforms
673 experienced multiple cycles of alluvial aggradation and incision since the early Pleistocene, but
674 most of these alluvial activities were confined within the massive incised valley that was created
675 during an episode of large-scale alluvial incision in the early Pleistocene (Figure 10). This valley
676 was, however, almost completely filled by reworked loess through continuous alluvial aggradation
677 by the middle phase of the late Pleistocene. The accreting river channel means that the river water
678 was closer to the surface of the terraces or tablelands which became prone to be inundated. Before
679 20000 BP, rivers in the region experienced another episode of alluvial incision, from which alluvial
680 terraces T4 emerged. This incision event was of a smaller scale compared to the early Pleistocene
681 one. Loose sediments blanketed on the incised river valley. By the terminal Pleistocene, a prolonged
682 period of alluvial accretion resumed and the river valleys were once again filled with alluvial
683 sediments, which were distributed widely in the region.

684 River downcutting began again from around 8000 BP. Narrow and shallow river valleys were
685 created during this small-scale alluvial incision. It also resulted in the formation of alluvial terraces
686 T3, which are most widely preserved today (Figure 10). In the ensuing event of river accretion
687 between 8000-4000 BP, major rivers such as the Shuangji River and their tributaries all experienced
688 siltation, which further shortened the height between the river water and surface of the alluvial
689 terraces T3. Along the edge of the alluvial terraces T3 and T4 some small-sized lakes and wetlands
690 appeared as the regional hydrological condition improved. By around 3500 BP, rivers began to incise
691 again and most lakes and wetlands on the alluvial terraces T3 and T4 gradually disappeared. This
692 large-scale river downcutting also eroded most of the alluvial terraces T2 along the Shuangji,
693 Zhenshui and other major rivers in the region. It was only on tablelands and low hills that parts of
694 the alluvial terraces T2 were preserved. The last stage of Holocene alluvial history witnessed another
695 cycle of alluvial incision-aggradation during the historical times, directly responsible for the
696 formation of modern river terraces T1.

697

698 Our research also suggested that the Shuangji River and Zhenshui River formed exceptionally
699 deep incised valleys in 30000-20000 a BP and 10000- 8000 a BP, coinciding with the formation of
700 alluvial terraces T4 and T3, respectively. The heights from the tops of the alluvial terraces T3 or T4
701 to their corresponding valley bottoms were very large. Although the river accretion narrowed the
702 heights during 8000-4000 a BP, channels of the Shuangji River, Zhenshui River and other major
703 regional rivers were confined within these deep valleys. These rivers never overflowed the tops of
704 alluvial terraces T3 and T4 again. At the same time, alluvial accretion also occurred in some tributary
705 gullies and led to the formation of many small lakes on the terraces. Such changes would have
706 provided an optimal hydrological condition conducive to growth of prehistoric settlements on the
707 terraces, which is discussed below.



724 Figure 10. Reconstruction of alluvial geomorphological evolution since the late Pleistocene

725 (**Pliocene epoch:** alluvial fan in the eastern foot of Songshan Mountain; **Early Pleistocene:** Large

726 deep valley were formed after a mass undercutting erosion; **30000 BP**: The valley was almost
727 filled in after a large scale accretion; **20000 BP**: New valley after a undercutting erosion emerged
728 again; **10000 BP**: small water areas appeared after an accretion; **8000 BP**: shallow valley appeared
729 after a undercutting erosion; **4000 BP**: water areas occurred after an accretion; **3000 BP**: deep
730 valley was formed after a mass undercutting erosion; **Modern**: present valley shape).

731

732

733 There is a correlation between evolution of alluvial landforms and Holocene climate change in
734 Shuangji River Basin. Recent speleothem $\delta^{18}\text{O}$ records in central China show weakened summer
735 monsoon events during the Holocene (Cai et al, 2021), including the so-called 8.2ka and 4.2ka
736 events, when the region experienced periods of climate variability. The development process of
737 Holocene alluvial terraces in Shuangji River valley roughly correspond to these climate events,
738 although the exact mechanisms responsible for this process are open to further scientific
739 investigations.

740 **5.2 Impact of alluvial landscapes on prehistoric settlement distributions**

741 The geomorphological changes reconstructed above are closely related to succession and
742 growth of prehistoric settlements in the Shuangji River Basin. Although the evolution of late
743 Pleistocene and Holocene alluvial landscapes is characterized by multiple cycles of alluvial incision
744 and aggradation, these events were of various magnitudes and scales and had different impact on
745 the geomorphological and ecological conditions of the region. The massive-scale early Pleistocene
746 alluvial incision profoundly shaped the geomorphological characteristics of the region. The hills and
747 valleys systems, separated by the remnant Neogene red-clay and boulders, became the
748 geomorphological spaces atop of which late Pleistocene and early Holocene alluvial terraces T4 and
749 T3 developed and evolved. Amongst these cyclic alluvial activities, those middle Holocene river
750 downcutting and aggradation events were of relatively smaller scale. Despite the extended episode
751 of the middle Holocene alluvial accretion, much of the surfaces of alluvial terraces T4 and T3 were
752 never inundated as we did not find traces of sediments that were related to floods on these surfaces,
753 contrary to Xia et al.'s suggestion (2003). However, as aforementioned, there existed many small
754 lakes and wetlands along small river valleys which were separated by loess belts and never

755 conjoined. They were fed by surface runoff flowing through the slopes and other landforms in the
756 valleys and overall did not cause disastrous impact on the surfaces of the alluvial terraces T4 and
757 T3. Such a dual stability of the middle-Holocene geomorphological and hydrological landscapes on
758 the alluvial terraces T4 and T3 was critical to the growth and expansion of prehistoric settlements
759 in the region.

760 Most Neolithic and Bronze-Age settlements were located on the surfaces of the alluvial
761 terraces T3, whilst some were scattered on those of the alluvial terraces T4. Even during the peak
762 of the middle Holocene event of protracted alluvial aggradation, the surfaces of the alluvial terraces
763 T4 remained 20 m higher than the river water, rendering them optimal places for prehistoric
764 occupation. Another beneficial factor was that, whilst such places were high up from river water,
765 there was abundant water in the small valleys and small lakes during the Holocene humid period
766 (also see [Chen FH et al, 2015](#); [Li GQ et al, 2020](#)), which provided sufficient water to the daily
767 consumption of the settlements and dryland agriculture. Although t the surfaces of the alluvial
768 terraces T3 were of relatively altitude, they were hardly inundated even during the maximum flood
769 level. This hydrological environment surrounding sites on the alluvial terraces T3 was convenient
770 to not only the expansion of mixed agriculture of millets and rice, but also to the construction of
771 large-scale water management facilities such as moats which were often connected to natural rivers.
772 Examples of the latter include moats at the Xinzhai and Guchengzhai sites. Because of the flat
773 terrains and optimal hydrological condition, the alluvial terraces T3 were occupied by a large
774 number of Neolithic to Bronze-Age settlements. Indeed, such favourable environmental conditions
775 sustained continuous growth and expansion of prehistoric settlements ([Lu et al, 2015](#)), culminating
776 with the rise of large-scale central walled towns by the late Longshan and Xinzhai period, including
777 such as the aforementioned Guchengzhai and Xinzhai sites where large-sized palaces were built
778 ([SACRCPU and ZICH, 2008](#); [Cai QF and Ma JC, 2002](#); [Zhang XH, 2019](#)). By the Xia-Shang period,
779 the pronounced rise of the Wangjinglou site with an enormous walled enclosures and other urban
780 infrastructures marked the unparalleled importance of this region in the civilizational discourse on
781 the Central Plains ([Gu, 2016](#)).

782

783 **5.3 Basin-scale landscape stability, prehistoric cultural developments and the emergence**

784 **of civilization on the Central Plains**

785 Several regions in prehistoric China were homes to many developed cultures, such as the
786 Ganqing region of the Upper Yellow River valley, the Haidai region in the Lower Yellow River
787 valley, the Sichuan Basin of the Upper Yangtze River valley, the Jiangnan Plain of the Middle
788 Yangtze River valley, and the Taihu Lake region of the Lower Yangtze River valley as well as the
789 West Liao River valley. Many of these early cultures experienced, however, a sudden decline or
790 collapse or were replaced or succeeded by other cultures during the late Holocene, coinciding with
791 some of the Holocene climate events (Su, 2009; Liu L, 1998; IACASS, 2010). Of the most notable
792 and well-studied example was the Lower Yangtze River, or more specifically, the Taihu Plain
793 surrounding the Yangtze Delta region. After the early venture into the low-lying coastal land by the
794 Kuahuqiao people (8000-7500 BP), the region saw an occupational hiatus until the Majiabang
795 culture period (7000-5900 BP). The continuous development of regional cultures, evidenced by the
796 dramatic increase of settlements and other factors such as intensified rice agriculture, culminated
797 during the Liangzhu culture period (5300-4300 BP) with the rise of an enormous city site with
798 developed urban and hydraulic infrastructures and magnificent material culture (Zhuang and Du,
799 2021). The rise and prosperity of the prehistoric cultures in the region were closely intertwined with
800 environmental change, especially Holocene sea-level fluctuations and associated geomorphological
801 development. As demonstrated by many studies, the emergence of land and improved hydrological
802 regimes in the region fostered the continuous development of the Majiabang, Songze (5900-5300
803 BP) and Liangzhu culture (Wang S et al, 2020; Jin et al, 2019). The decline of the Liangzhu culture
804 has now also been popularly linked to the late-Holocene climate and environmental change on the
805 Yangtze Delta region. The widespread presence of the yellowish flood deposits, directly
806 superimposing the Liangzhu layer, is considered as one of the most direct evidence that region-wide
807 floods contributed to the demise of the Liangzhu Civilization (He et al, 2019), along with other
808 reasons. Compared to such ebbs and flows of prehistoric cultures in the Yangtze Delta region, the
809 Central Plains of the Middle Yellow River experienced a remarkable continuum of development of
810 prehistoric cultures. Such a developmental trajectory is considered to be a representative of the
811 unification and continuity of the Chinese civilization. Whilst many factors acted in concert to shape
812 such a unique characteristic of prehistoric culture development on the Central Plains, the prolonged

813 stability of the middle to late Holocene landscape also played a key role in this process.

814 Situated between the Loess Plateau and the North China Plain, the geomorphological
815 characteristics of the Central Plains are shaped by both loess accumulation and alluvial processes.
816 Loess tablelands are one of the most prevalent landforms in the region. Such geomorphological
817 units are often situated on high-altitude place with a flat and broad surface which continues to
818 receive wind-blown loess throughout the late Pleistocene to Holocene. Specifically, according to the
819 geomorphological history of the Shuangji River, the loess tablelands can be divided into several
820 categories according to their altitudes, sediments and chronologies. These include low-rising river
821 terraces, high-altitude river terraces and tablelands, all suitable for prehistoric occupation.
822 Prehistoric communities living on these places adapted to different hydrological and
823 geomorphological conditions. The low rising river terraces were particularly attractive places to the
824 prehistoric communities as they provided ample water resources whilst also keeping away from
825 floods. Agriculture flourished on these low-rising fertile lands and gradually advanced forms of
826 water management facilities were also built. These would have been an important precondition for
827 the steady and continuous cultural developments of the Central Plains region, and for its eventual
828 rise as a one of the most typical cultural entities of the Chinese civilization.

829 Despite being a relatively small-sized river basin, the Shuangji River valley and its diverse
830 landforms experienced almost uniform and synchronous geomorphological changes during the
831 Holocene, especially during the middle to late Holocene. Such a synchronicity and stability of
832 Holocene alluvial landscapes are related to several geological and environmental factors. First, the
833 massive-scale early Pleistocene river downcutting shaped the backbone of the region's Quaternary
834 environment and as we have demonstrated above, most geomorphological processes were confined
835 within the space of the Pleistocene river valley. Second, the tempo and scale of alluvial aggradation
836 and incision are also inherently related to the properties of loess which continues to accumulate
837 during the Holocene and is easy to be reworked through alluvial processes. Coupled with the fact
838 that loess is well known for its fertility to agricultural production and the stable hydrological
839 condition on the loess landscapes, the Shuangji River sustained continuous cultural developments
840 on the Central Plains and the unique human-environment interaction in the basin also profoundly
841 defined the developmental trajectories of the Chinese Civilization. In the dramatic cultural changes

842 and environmental vagaries during the late Holocene, the landscape stability in the Shuangji River
843 basin became an even more advantageous factor in fostering the emergence of Chinese civilization
844 on the Central Plains whilst cultures in other contemporary regions declined.

845

846 **6. Conclusion**

847 Evolution of alluvial geomorphology during the Holocene in the Shuangji River Basin of the
848 Central Plains is reconstructed by multi-scalar evidence derived from our field surveys and
849 laboratory analyses of the sediment and dating samples. Our results show that the Neogene alluvial
850 fan was incised into a wide valley by the river during the early Pleistocene. This wide valley
851 constituted the geomorphological space that reframed regional alluvial processes. About 20, 000 BP
852 and 10,000-8,000 BP, regional rivers started to incise the loess landform again and created the
853 alluvial terraces T4 and T3, respectively. These alluvial terraces maintained an overall remarkable
854 stability, withstanding subsequent geomorphological processes, and became the main arena of
855 successive prehistoric to Bronze-Age human occupation. Since then, these alluvial terraces were, to
856 a large extent, free from the impact of large-scale floods even during the large-scale alluvial siltation
857 during 8,000-3,000 BP. Amongst many other factors, the stability of the Holocene landscape,
858 especially those locations such as alluvial terraces and loess tablelands with optimal hydrological
859 and soil conditions was one of the most fundamental factors that contributed to the steady settlement
860 and population growth and intensifying agricultural production. These laid an important foundation
861 for the prehistoric cultural development in Shuangji River Basin and contributed to the unparalleled
862 cultural continuity on the Central Plains.

863

864 **Acknowledgements**

865 The study is funded by the National Key R&D Program of China(2020YFC1521605), the
866 National Natural Science Foundation of China (Grant Nos. 41971016, 41671014 and 42071119),
867 the National Social Science Foundation of China (Grant Nos. 18CKG003 19ZDA227), Science and
868 Technology Project of Henan Province (Grant No. 192102310019), Soft Science Research Project
869 of Henan Province (Grant No. 192400410067), the Study of Environment archaeology in
870 Zhengzhou, the Digital Environment Archaeology Specially-appointed Researcher of Henan, China

871 (Grant No. 210501002), and the Research on the Roots of Chinese Civilization of Zhengzhou
872 University (XKZDJC202006), and the Science and technology open cooperation project
873 (210901006) and Science and Technology Think-Tank Project of Henan Academy of Sciences
874 (Grant No. 210701002).

875

876 **Reference**

877 Bestel S, Bao Y, Zhong H, Chen XC, Liu L. 2017. Wild plant use and multi-cropping at the
878 early Neolithic Zhuzhai site in the middle Yellow River region, China. *The Holocene*. 28(2), 195–
879 207.

880 Bullock, P., Fedoroff, N., Jongerius, A., Stoops, G., Tursina, T., 1985. Handbook for Soil Thin
881 Section Description. Waine Research Publications, Wolverhampton.

882 Brown AG. 1997. Alluvial geoarchaeology, floodplain archaeology and environmental change.
883 Cambridge: Cambridge University Press.

884 Cai QF and Ma JC. 2002. Excavation of Guchengzhai City Site of Longshan Culture in Xinmi
885 City of Henan Province. *Huaxia Archaeology*. (2): 53-82. (in Chinese with English abstract).

886 Cai YJ, Cheng X, Ma L, et al. 2021. Holocene variability of East Asian summer monsoon as
887 viewed from the speleothem $\delta^{18}O$ records in central China. *Earth and Planetary Science Letters*,
888 <https://doi.org/10.1016/j.epsl.2021.116758>.

889 Chen FH, Xu Q H, Chen JH et al. 2015. East Asian summer monsoon precipitation variability
890 since the last deglaciation. *Scientific Reports*, 5: 11186.

891 Colin Renfrew and Paul Bahn, 2012. *Archaeology, Theories, Methods and Practice*. London,
892 Thames & Hodson Ltd.

893 Deng Z, Fuller DQ, Chu X, Cao Y, Jiang Y, Wang L, Lu H. 2019. Assessing the occurrence and
894 status of wheat in late Neolithic central China: the importance of direct AMS radiocarbon dates from
895 Xiashai. *Vegetation History and Archaeobotany*. doi:10.1007/s00334-00019-00732-00337.

896 Giosan L, Clift PD, Macklin MG et al. 2012. Fluvial landscapes of the Harappan civilization.
897 *PNAS*. www.pnas.org/cgi/doi/10.1073/pnas.1112743109.

898 Gu WF. 2016. *Xinzheng Wangjinglou-the Field archaeological excavation during 2010-2012*.
899 Beijing: Science Press. (in Chinese)

900 He K, Lu H, Sun G, Ji X, Wang Y, Yan K, Zuo X, Zhang J, Liu B, Wang N. 2021. Multi-proxy
901 evidence of environmental change related to collapse of the Liangzhu Culture in the Yangtze Delta,
902 China. *Science China Earth Sciences*, 64(6): 890–905, <https://doi.org/10.1007/s11430-020-9767-5>.

903 IACASS, 2010. *Chinese Archaeology-Neolithic*. Beijing: China Social Sciences Press. (in
904 Chinese).

905 Jiang FC, Wu XH, Xiao HG, Wang SM, Xue B. 1997. The High resolution late Pleistocene
906 loess stratigraphy in Taohuayu, Mangshan, Zhengzhou. *Journal of Geomechanics*, 3(2): 11-17. (in
907 Chinese with English abstract).

908 Jin Y, Mo D, Li Y, Ding P, Zong Y, Zhuang Y. 2019. Ecology and hydrology of early rice
909 farming: geoarchaeological and palaeo-ecological evidence from the Late Holocene paddy field site
910 at Maoshan, the Lower Yangtze. *Archaeological and Anthropological Sciences*, 11:1851–1863.
911 <https://doi.org/10.1007/s12520-018-0639-1>

912 Kidder TR, Katherine AA, Lee JA, Timothy MS. 2008. Basin-scale reconstruction of the
913 geological context of human settlement: an example from the lower Mississippi Valley, USA.
914 *Quaternary Science Reviews*. 27: 1255 – 1270.

915 Kidder T, Liu H, Xu Q, Li M. 2012. The alluvial geoarchaeology of the Sanyangzhuang site
916 on the Yellow River floodplain, Henan Province, China. *Geoarchaeology* 27:324-343.

917 Kidder TR, Zhuang Y. 2015. Anthropocene archaeology of the Yellow River, China, 5000–
918 2000 BP. *The Holocene* 25:1627-1639.

919 Li GQ, Wang Z, Zhao WW, et al. 2020. Quantitative precipitation reconstructions from Chagan
920 Nur revealed lag response of East Asian summer monsoon precipitation to summer insolation during
921 the Holocene in arid northern China. *Quaternary Science Reviews*.
922 <https://doi.org/10.1016/j.quascirev.2020.106365>.

923 Li YQ, Chen XC, Gu WF, et al. 2020. Excavation of Peiligang Site in Xinzheng of Henan
924 during 2018-2019. *Acta Archeologica*. (4): 521-546. (in Chinese)

925 Liao, Y., Lu, P., Mo, D., Wang, H., Storozum, M.J., Chen, P., Xu, J., 2019. Landforms influence
926 the development of ancient agriculture in the Songshan area, central China. *Quaternary International*
927 521, 85–89.

928 Liu L. 1998. Chiefdoms and Settlement Forms of Longshan Culture. *Huaxia Archaeology*, (1):

929 88-105. (in Chinese)

930 Liu L and Chen XC. 2017. The archaeology of China, from the late Paleolithic to the early
931 Bronze Age. Beijing: SDX Joint Publishing Company. (in Chinese)

932 Liu QZ and Han GH. 2016. The archaeological observation on the evolution of the history and
933 culture in the central plains area. *Acta Archaeologica Sinica*. (3): 293-318. (in Chinese)

934 Lu, P.; Tian, Y. The successive mode of 9000–3000 aB.P. settlements and its relationship with
935 the terrain around Songshan Mountain. *Quaternary Science*. 2013, 33, 965–971. (In Chinese)

936 Lu P, Tian Y, Yang R X. 2013b. The study of size-grade of prehistoric settlement in the Circum-
937 Songshan area based on SOFM network. *Journal of Geographical Sciences*, 23 (3): 538-548.

938 Lu P, Mo DW, Wang H, Yang RX, Tian Y, Chen PP, Lasaponara R, Masini N. 2017. On the
939 Relationship between Holocene Geomorphological Evolution of Rivers and Prehistoric Settlements
940 Distribution in the Songshan Mountain Region of China, *Sustainability*, 9, 114;
941 doi:10.3390/su9010114.

942 Lu, P., Chen, P., Tian, Y., He, Y., Mo, D., Yang, R., Lasaponara, R., Masini, N., 2019a.
943 Reconstructing settlement evolution from neolithic to Shang dynasty in Songshan mountain area of
944 central China based on self-organizing feature map. *Journal of Cultural Heritage* 36, 23–31.

945 Lu, P., Wang, H., Chen, P., Storozum, M.J., Xu, J., Tian, Y., Mo, D., Wang, S., He, Y., Yan, L.,
946 2019b. The impact of Holocene alluvial landscape evolution on an ancient settlement in the
947 southeastern piedmont of Songshan Mountain, Central China: A study from the Shiyuan site. *Catena*
948 183, 104232.

949 Lu P, Lv JQ, Zhuang YJ, Chen PP, Wang H, Tian Y, Mo DW, Xu JJ, Gu WF, Hu YY, Wei QL,
950 Yan LJ, Wang X, Zhai HG. 2021. Evolution of Holocene alluvial landscapes in the northeastern
951 Songshan Region, Central China: Chronology, models and socio-economic impact. *Catena*.
952 <https://doi.org/10.1016/j.catena.2020.104956>.

953 Macklin MG, Woodward J C, Welsby D A, Duller G A T, Williams FM, Williams M A J. 2013.
954 Reach-scale river dynamics moderate the impact of rapid Holocene climate change on floodwater
955 farming in the desert Nile. *Geology*, 41(6): 695–698.

956 Macklin MG, Willem HJ, Jamie TC. Woodward, Williams MAJ, Flaux C, Marriner N, Nicoll
957 K, Verstraeten G, Spencer N, Welsby D. 2015. A new model of river dynamics, hydroclimatic

958 change and human settlement in the Nile Valley derived from meta-analysis of the Holocene fluvial
959 archive. *Quaternary Science Reviews*, <http://dx.doi.org/10.1016/j.quascirev.2015.09.024>.

960 Murphy, C.P., 1986. *Thin Section Preparation of Soils and Sediments*. A B Academic Publ.,
961 Berkhamsted.

962 Murray A S, Wintle A G. 2003. The single aliquot regenerative dose protocol: Potential for
963 improvements in reliability. *Radiation Measurements*, 37(4-5): 377-381.

964 Pang JL, Huang CC, Zha XC, Zhu YZ. 2008. Micro-morphological Features of Particles of
965 Holocene loess at Zhengzhou area, China and their environmental significance, 28(5): 683-687. (In
966 Chinese with English abstract)

967 Qu TL, Gu WF, Wang SZ, et al. 2018. Subsistence in the Middle Upper Pleistocene of
968 Zhengzhou area: Analysis of archaeofauna from the Laonainaimiao Site. *Acta Anthropologica*
969 *Sinica*, 37(1): 70-78. (in Chinese)

970 Ramsey Bronk, C. 1995. Radiocarbon calibration and analysis of stratigraphy: the OxCal
971 program. *Radiocarbon* 37:425-430.

972 Reimer PJ et al. 2020a. The IntCal20 Northern Hemisphere radiocarbon age calibration curve
973 (0–55 cal kBP). *Radiocarbon* 62:725-757.

974 Reimer PJ. 2020b. Composition and consequences of the IntCal20 radiocarbon calibration
975 curve. *Quaternary Research*. 96, 22–27. <https://doi.org/10.1017/qua.2020.42>.

976 RGSTHGB. 1987. *Geological map of the People's Republic of China -- Xuchang map*. Beijing:
977 China geological drawing printing factory. (in Chinese)

978 SACRCPU and ZICH. 2008. *Xinmi Xinzhai- the Field archaeological excavation during 1999-*
979 *2000*. Beijing: Cultural Relics Press. (in Chinese)

980 Stoops, G., 2003. *Guidelines for Analysis and Description of Soil and Regolith Thin Sections*.
981 Soil Science Society of America, Wisconsin.

982 Su BQ. 2009. *New exploration on the origin of Chinese civilization*. Shenyang: Liaoning
983 People's Publishing House. (in Chinese)

984 Wang, C., 2016. *Research on the early farming-human activities in the central China and their*
985 *relation with climate change*. University of Chinese Academy of Sciences. (in Chinese with English
986 abstract).

987 Wang, C., Lu, H., Gu, W., Wu, N., Zhang, J., Zuo, X., Hu, Y. 2017a. The spatial pattern of
988 farming and factors influencing it during the Peiligang culture period in the middle Yellow River
989 valley, China. *Science Bulletin* 62(23), 1565–1568.

990 Wang, C., Lu, H., Gu, W., Zuo, X., Zhang, J., Liu, Y., Hu, Y. 2017b. Temporal changes of mixed
991 millet and rice agriculture in Neolithic-Bronze Age Central Plain, China: Archaeobotanical evidence
992 from the Zhuzhai site. *The Holocene*, 28(5), 738–754.

993 Wang H. 2007. A preliminary study on the relationship between the changes of settlement
994 distribution and natural environment in the Neolithic Age in the middle-upper reaches of Shuangji
995 River. In CSTAIACASS edit. *Science and Technology Archaeology (Series II)*. Beijing: Science
996 Press, 141-154. (in Chinese)

997 Wang H, Lu P, Xu JJ, Mo DW. 2019. Discussion on the role of the natural environment in the
998 production mode- a case from the Neolithic Zhenshui River Basin in Henan. *Cultural Relics in*
999 *Southern China*. (5): 170-179. (in Chinese with English abstract).

1000 Wang S, Ge J, Kilbourne KH, Wang Z. 2020. Numerical simulation of mid-Holocene tidal
1001 regime and storm-tide inundation in the south Yangtze coastal plain, East China. *Marine Geology*,
1002 423: 106134. <https://doi.org/10.1016/j.margeo.2020.106134>.

1003 Wang YP, Zhang SL, He JN, Wang SZ, Zhao JF, Qu TL, Wang JY, Gao XX. 2011 Excavation
1004 of Lijiagou Site in Xinmi, Henan Province. *Archaeology*, (4): 291-297.

1005 Wang YP. 2013. Hominid habitat patterns and its related problems in Mis3 stage at the
1006 southeastern piedmont of Songshan Mountain. In *Archaeology and Museology College of Peking*
1007 *University and Chinese Archaeological Research Center of Peking University edit. Archaeological*
1008 *Research* (10). Beijing: Science Press, 287-296. (in Chinese)

1009 Wang YP, Xia ZK, Wang SZ. 2018. Lijiagou Site and the transition of Paleolithic-Neolithic
1010 Age-Research on agricultural origin in the east piedmont of Songshan Mountain. Beijing: Science
1011 Press. (in Chinese)

1012 Xia ZK, Wang ZH, Zhao CQ. 2003. Abnormal flood events and the climatic background
1013 around 3500 aBP in Central China. *Science in China (Series D)*. 33 (9): 881-888. (in Chinese with
1014 English abstract)

1015 Yan WM. 1987. The unity and diversity of Chinese prehistoric culture. *Cultural Relics*. (3): 38-

1016 50. (in Chinese)

1017 Yang YM, Huang CC, Pang JL. 2005. Source of the Holocene Aeolian loess-Soil in the upper
1018 reaches of the Huai River. *Geography and Geo-information Science.*, 21(1): 43-46. (In Chinese with
1019 English abstract)

1020

1021 Yao ZQ, Wu Y, Wang CS, Zhao CQ. 2007. Analysis of phytolith in Xinzhai Site, Xinmi City,
1022 Henan Province. *Archeology.* (3): 90-96. (in Chinese with English abstract).

1023 Yu S, Zhu C, Song J, Qu WJB. 2000. Role of climate in the rise and fall of Neolithic cultures
1024 on the Yangtze Delta. *Boreas.* 29:157-165.

1025 Yu SY, Hou ZF, Chen XX, et al. 2020. Extreme flooding of the lower Yellow River near the
1026 Northgrippian-Meghalayan boundary: Evidence from the Shilipu archaeological site in
1027 southwestern Shandong Province, China. 350:106878.

1028 Zhang, J. F., Qiu, W. L., Wang, X. Q., Gang, H., Li, R. Q., & Zhou, L. P. 2010. Optical dating
1029 of a hyperconcentrated flow deposit on a yellow river terrace in hukou, shaanxi, china. *Quaternary*
1030 *Geochronology*, 5(2-3), 194-199.

1031 Zhang JP, Lu HY, Gu WF, Wu NX, Zhou KS, Hu YY, Wang C. 2012. Early mixed farming of
1032 millet and rice 7800 years ago in the middle Yellow River region, China. *PLoS ONE.* 7(12), e52146.

1033 Zhang XH. 2019. Excavation of Guchengzhai Site in Xinmi of Henan during 2016-2017.
1034 *Huaxia Archaeology.* (4): 3-13. (in Chinese)

1035 Zhang ZY, Zhou K S, Yang R X, Zhang SL, Cai QF, Lu P, Hao LM, Wang C. 2007.
1036 Environmental archaeology in the Shuangji River Basin. *Quaternary Sciences*, 27(3): 453-460. (In
1037 Chinese).

1038 Zhao Z J. 2011. New archaeobotanic data for the study of the origins of agriculture in China.
1039 *Current Anthropology.* 52(4): 295–306.

1040 Zheng Y, Yu SY, Fan T, et al. 2021. Prolonged cooling interrupted the Bronze Age cultures in
1041 northeastern China 3500 years ago. *Palaeogeography, Palaeoclimatology, Palaeoecology*
1042 574:110461.

1043 Zhou KS, Zhang SL, Zhang ZY et al. 2005. Songshan Mountain Culture Circle. *Cultural Relics*
1044 of Central China. (1): 12-20. (in Chinese).

1045 Zhuang Y, Kidder TR. 2014. Archaeology of the Anthropocene in the Yellow River region,
1046 China, 8000–2000 cal. BP. *The Holocene* 24:1602-1623.

1047 Zhuang Y and Du S. 2021. Holocene sea-level change and evolution of prehistoric settlements
1048 around the Yangtze Delta region// *Palaeolandscapes in Archaeology*, 192-214. Routledge.
1049 [https://www.routledge.com/Liangzhu-Culture-Society-Belief-and-Art-in-Neolithic-](https://www.routledge.com/Liangzhu-Culture-Society-Belief-and-Art-in-Neolithic-China/author/p/book/9781138557406)
1050 [China/author/p/book/9781138557406](https://www.routledge.com/Liangzhu-Culture-Society-Belief-and-Art-in-Neolithic-China/author/p/book/9781138557406)

1051

1052

1053

1054